

https://dspace.org/

Fenofibrate prevents isoproterenol-induced left ventricular hypertrophy and pump dysfunction in rats

Maswanganyi, Tlangelani

2011-01-31
http://hdl.handle.net/10539/8991

Downloaded from a DSpace repository. https://dspace.org/

1. INTRODUCTION

1.1. Epidemiology of cardiac hypertrophy and heart failure

Epidemiological data suggest that the number of cases of patients with heart failure increases by approximately 700 000 every year in the United States of America (Heart Failure Society of America practice guidelines, 1999). The number of cases of heart failure continues to increase despite improved treatment regimens as evidenced by an increase in the number of admissions of patients with heart failure (Roger et al 2004 and Juenger et al 2002). The exponential rise in the incidence of heart failure is expected to match with a proportionate rise in future health care costs (Heart Failure Society of America practice guidelines, 1999).

Hypertension, diabetes mellitus and obesity are recognised as clinical risk factors of both concentric and dilated heart failure (Levy et al 1996, Iribarrenet et al 2001 and Kenchaiah et al 2004). The probability of deaths arising from cardiac complications increases by two to four times in patients with left ventricular hypertrophy (LVH) (Levy et al 1990). The rate of mortality caused by heart failure is increased five-times in patients with diabetes mellitus (Iribarrenet et al 2001). Although not fully understood, the risk of mortality among heart failure patients is also thought to be increased in obese patients (Shocken et al 2008). These studies support the notion that hypertension, diabetes mellitus and obesity are strongly associated with LVH and left ventricular (LV) systolic chamber dysfunction. Other risk factors such as smoking, alcohol abuse and chronic renal failure are considered less consequential in predicting mortality caused by heart failure (Walsh et al 2002, Eliasson et al 2003 and Fried et al 2003).

Hypertension causes heart failure by inducing LVH (Lavie et al 1992). When exposed to high blood pressures, the heart compensates by increasing left ventricular mass (LVM) in order to

maintain pump function; this increase in LVM becomes pathologic at a certain point by causing impairment of LV filling and therefore diastolic dysfunction (Schillaci et al 2000). Thus, LVH may be advantageous in early stages of heart failure by enabling the heart to maintain haemodynamic function; however, sustained insult is regarded as a significant contributor to functional decline in heart failure (Seymour, 2003). Clinical studies suggest that LVH is the main predictor of mortality in cardiac complications (Casale et al 1986 and Koren et al 1991). In the United Kingdom alone, at least 69% of concentric heart failure cases are associated with hypertension (Hawkins et al 2007). Also, LVH has strongly been associated with metabolic disorders such as diabetes mellitus and obesity (Lee et al 1997 and Lavie et al 1988). Thus, a metabolic approach to heart failure therapy may be a viable alternative (Opie et al 2006). Although the role of metabolic remodelling in heart failure is still not completely understood, evidence is accumulating that changes in metabolic regulation contribute significantly to LV remodelling and dysfunction (Lee et al 2005; Fragasso et al 2006 and Brigadeau et al 2007).

1.2. Normal cardiac metabolism

In the adult heart, fatty acid oxidation (FAO) is regarded as the main source of energy needed for normal function since FAO accounts for at least 60% of cardiac energy production; 35% of cardiac energy is produced from glucose metabolism while the metabolism of amino acids and ketone bodies accounts for the remaining 5% (Wisneski et al 1985 and Bing et al 1954). Primarily, FAO mostly occurs in mitochondria while a small fraction of FAO i.e. the breakdown of very long chain fatty acids into long chain fatty acids occurs in peroxisomes (Schulz, 1994). The uptake of free fatty acids (FFAs) from the circulation into cardiomyocytes can either occur

inactively through diffusion (i.e. medium chain fatty acids) or is facilitated by transport proteins such as fatty acid translocase (FAT) and fatty acid binding protein (FABP) i.e. long chain fatty acids (Glatz et al 2001 and Van der Vusse et al 2000). In the cytosol, fatty acyl-co-enzyme A (CoA) synthase (FACS) catalyzes the esterification of FAs to fatty acyl-coA, thereby enabling mitochondrial FA transport (Schaffer, 2002). Carnitine is responsible for the transport of fatty acyl-CoA across the mitochondrial membrane. Fatty acyl CoA attaches to carnitine forming fatty acyl carnitine in a reaction facilitated by the enzyme carnitine palmitoyl transferase 1 (CPT-1), located in the outer mitochondrial membrane (OMM). Carnitine acyl translocase then facilitates the passage of fatty acyl-CoA through the inner mitochondrial membrane (IMM) and the return of carnitine to the OMM; carnitine palmitoyl transferase 2 (CPT-2), located in the IMM catalyzes the re-formation of fatty acyl-CoA inside the mitochondrial matrix (Lopaschuk et al 1994; Kerner and Hoppel, 2000).

In the mitochondrion, fatty acyl-CoA undergoes β-oxidation by medium-chain acyl-CoA dehydrogenase (MCAD) and long-chain acyl-CoA dehydrogenase (LCAD) wherein it is converted to $NADH+H^+$, $FADH_2$ and acetyl Co-A. $NADH+H^+$ and $FADH_2$ electrons enter the mitochondrial electron transport chain (ETC) directly, while acetyl CoA goes into the tricarboxylic acid (TCA) cycle where it is oxidized to generate more $NADH+H^+$ and $FADH_2$. An electrochemical proton gradient between the mitochondrial matrix and inside of intermembrane space is created, enabling the movement of protons from the matrix into the intermembrane space of the mitochondrion. Electron transport chain is positioned on the inner mitochondrial membrane and made up of complexes I-IV**:** complex I (NADH coenzyme Q reductase) collects electrons from NADH and transfers them to coenzyme Q; electrons from complex II (succinate dehydrogenase) are also transferred to coenzyme Q, which carries these

electrons to complex III (cytochrome bc_1 complex. Complex III transfers electrons to cytochrome and cytochrome c enables entrance of electrons to complex IV (cytochrome c oxidase), a final electron acceptor. Complex IV also traps molecular oxygen, leading to formation of water (Murray et al 2003). Complex V (adenosine triphosphate (ATP) synthase) then facilitates the re-entry of protons into the mitochondrial matrix. In the process, ATP synthase uses the kinetic energy generated by the electrochemical proton gradient to ultimately synthesize ATP (Brownlee, 2001 and Stryler, 1999). At least 60% of ATP accessible to the heart gets used for contractile processes, while approximately 40% is used by ion pumps such as sarcoplasmic reticulum Ca^{2+}-ATPase (Suga, 1990). A summary of the processes involved in the catabolism of FAs is illustrated in figure 1.

1.2.1. Regulation of cardiac metabolism by AMP-activated protein kinase

AMP-activated protein kinase (AMPK) is said to function as a "gauge" that switches on during low energetic capacity in cells and is associated with increased expression of genes involved in energy generation (Bergeron et al 2001). AMPK is composed of three subunits, namely alpha, beta and lambda (Carling et al 2004). The alpha subunit is subdivided into α_1 and α_2; most tissues express α_1, while α_2 is mainly found in cardiac and skeletal muscle (Corton et al 1994). AMPKα_2 is found in nuclei of most cells. AMPK exerts its effects by influencing nuclear gene transcription and replication (Salt et al 1998). AMPKα_2 induces translocation of glucose transporter (GLUT-4) to sarcolemmal membrane, thereby stimulating cellular glucose uptake and thus glucose oxidation (Yamaguchi et al 2005). Upon activation, AMPKα_2 also reduces production of malonyl CoA by inhibiting acetyl-CoA carboxylase beta (ACCβ); since malonyl

CoA binds and inhibits CPT-1 thereby allowing increased uptake of FFAs into mitochondria for FAO (Stuck et al 2008). Thus, AMPKα_2 has a dual role since it can increase both fatty acid (FA) and glucose oxidation.

AMPKα_2 is stimulated by an increase in the ratio of AMP/ATP in the heart (Tian et al 2001 and Ponticos et al 1998). Studies have shown that AMPKα_2 stimulates energy production and inhibits energy-consuming processes such as protein synthesis (Hardie, 2003 and Horman et al 2002). Further, AMPKα_2 plays an important role in cardiac FA transport since it enhances translocation of FAT/CD36 sarcolemmal membrane (Luiken et al 2003). A summary of the regulation of cardiac metabolism by AMPK is illustrated in figure 2.

1.2.2. Transcriptional regulation of fatty acid metabolism

Peroxisome proliferator-activated receptors (PPARs) are a set of nuclear receptors that transcriptionally regulate processes such as cellular differentiation, development and metabolism in tissues (Feige et al 2006 and Berger and Moller, 2002). The PPAR family is divided into alpha, gamma and delta. Of these, the activity of PPARα tends to be greatest in tissues that require a high rate of metabolic energy production such as the liver and heart (Feige et al 2006 and Braissant et al 1996). PPARα regulates transcription of FAO genes by binding to a fatty acid response element (FARE) in the promoter regions of these genes (Gulick, 1994). PPARα controls target gene transcription via heterodimerization with retinoid X receptor (RXR) (Mangelsdorf and Evans, 1995). PPARα actions are enhanced by its co-activator peroxisome proliferator-activated receptor gamma coactivator- 1 alpha (PGC-1α) in cardiac muscle;

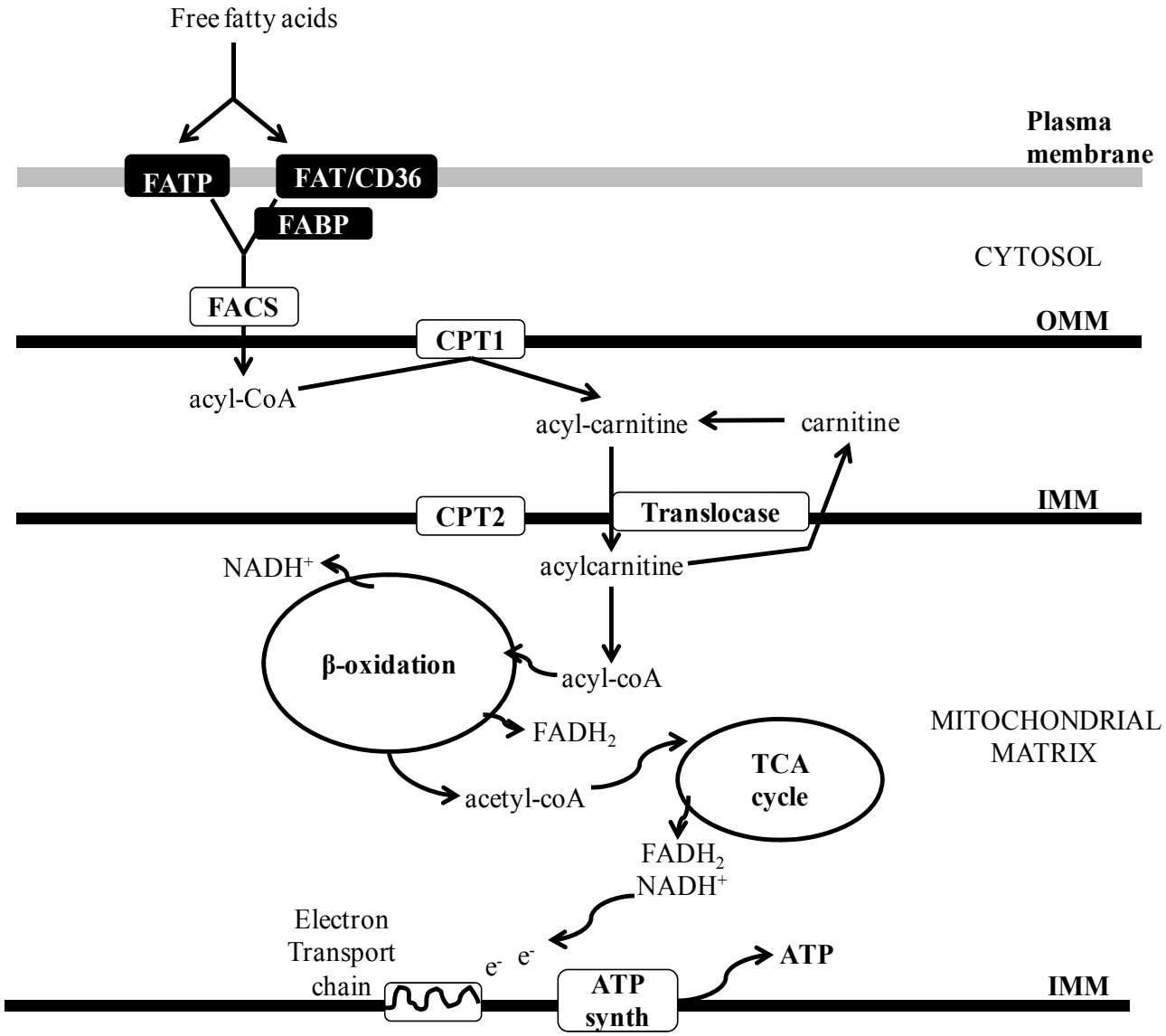

Figure 1. Fatty acid uptake, transport and mitochondrial β-oxidation. *OMM indicates outer mitochondrial membrane; IMM, inner mitochondrial membrane; FATP, fatty acid transport protein; FAT/CD36, fatty acid translocase/CD36; FABP, fatty acid binding protein; FACS, fatty acyl-CoA synthase; CPT, carnitine palmitoyl transferase; TCA, tricarboxylic acid.* ***Figure adapted from Barger and Kelly, 2000.***

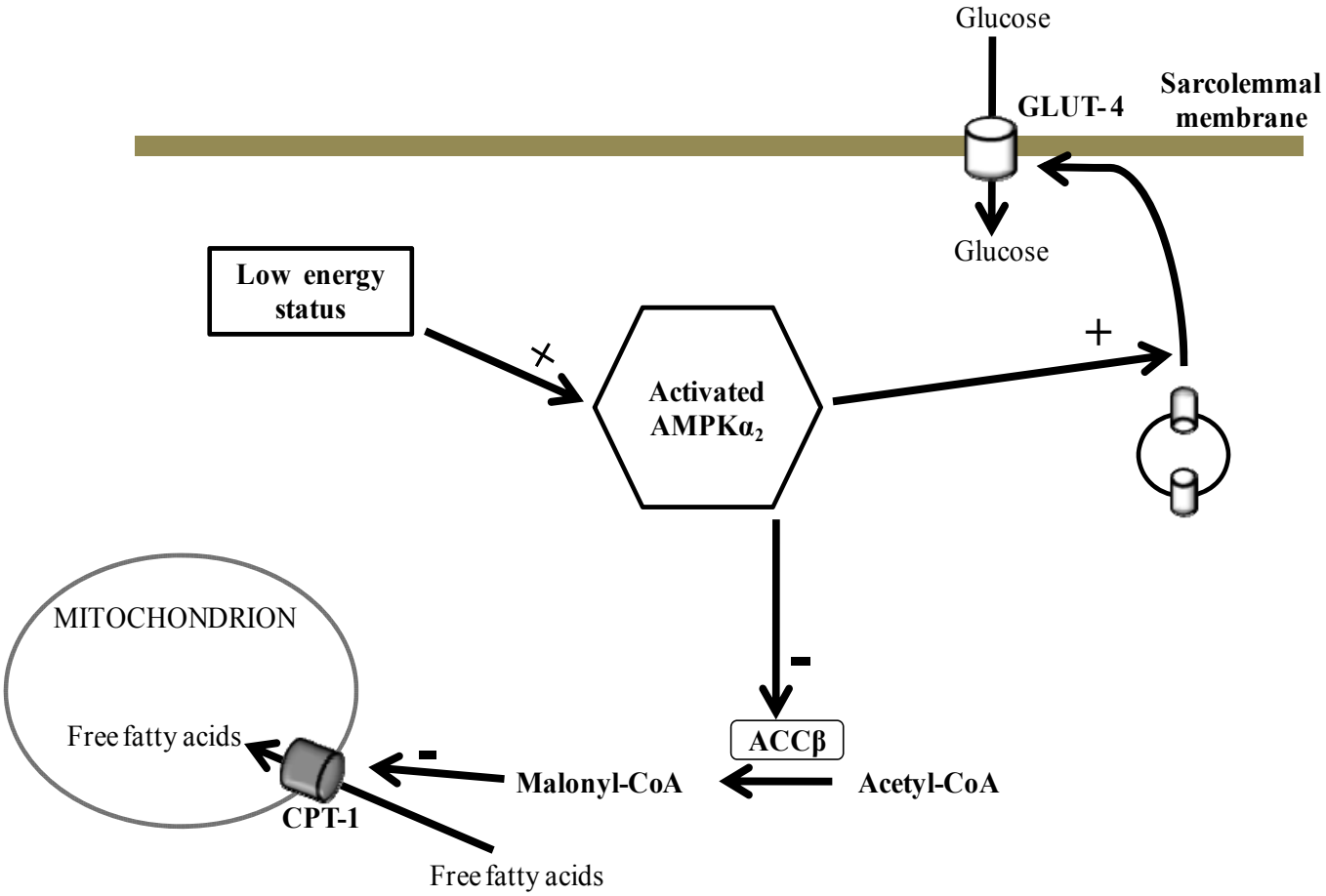

Figure 2. Regulation of fatty acid and glucose metabolism by AMPKα$_2$ in the heart. AMPKα$_2$ *indicates AMP-activated protein kinase alpha-2; GLUT-4, glucose transporter-4; ACCβ, acetyl CoA carboxylase-beta; CPT-1, carnitine palmitoyl transferase-1.*

on the other hand, AMPKα_2 activity stimulates PGC-1α in skeletal muscle (Zong et al 2002 and Vega et al 2000).

PPARα activation stimulates the expression of proteins/enzymes involved in FA transport such as FATP, FAT/CD36, FABP and acyl-CoA synthetase (ACS) (Motojima et al 1998 and Ibrahimim et al 1996); mitochondrial FA uptake, CPT-1 (Osorio et al 2002, Lionetti et al 2005 and Schaffer, 2003); and mitochondrial FAO such as medium chain acyl-CoA dehydrogenase (MCAD), long-chain acvl-CoA dehydrogenase (LCAD) and very long-chain acyl-CoA dehydrogenase (VLCAD) (Djouadi, 1999 and Gulick, 1994). PPARα expression is activated by long chain FFAs, which are natural ligands for activation of PPARα (Brandt et al 1998). Other than activation by FFAs, PPARα can also be activated by synthetic ligands such fenofibrate and WY-14643. Fenofibrate is predominantly used clinically to treat hyperlipidaemia (Forman et al 1997). A summary of the processes involved in the transcriptional control of FAO genes is illustrated in figure 3.

Lately, consequences of deletion of PPARα in mice have been studied; primarily, deletion of PPARα in mice induced downregulation of liver FAO enzyme expression (Lee et al 1995). Follow-up studies of mice with deletion of PPARα also revealed downregulation of FAO enzymes such as MCAD and CPT-1 in the heart (Djouadi et al 1998).

Peroxisome proliferator-activated receptor gamma coactivator (PGC) is a set of transcriptional coactivators that is divided into PGC-1α, PGC-1β and PGC-related coactivator (PRC) (Izquierdo et al 1995). PGC-1α is a chief regulator of mitochondrial biogenesis. Mitochondrial proliferation that occurs after birth requires upregulation of PGC-1α (Russell et al 2004a).

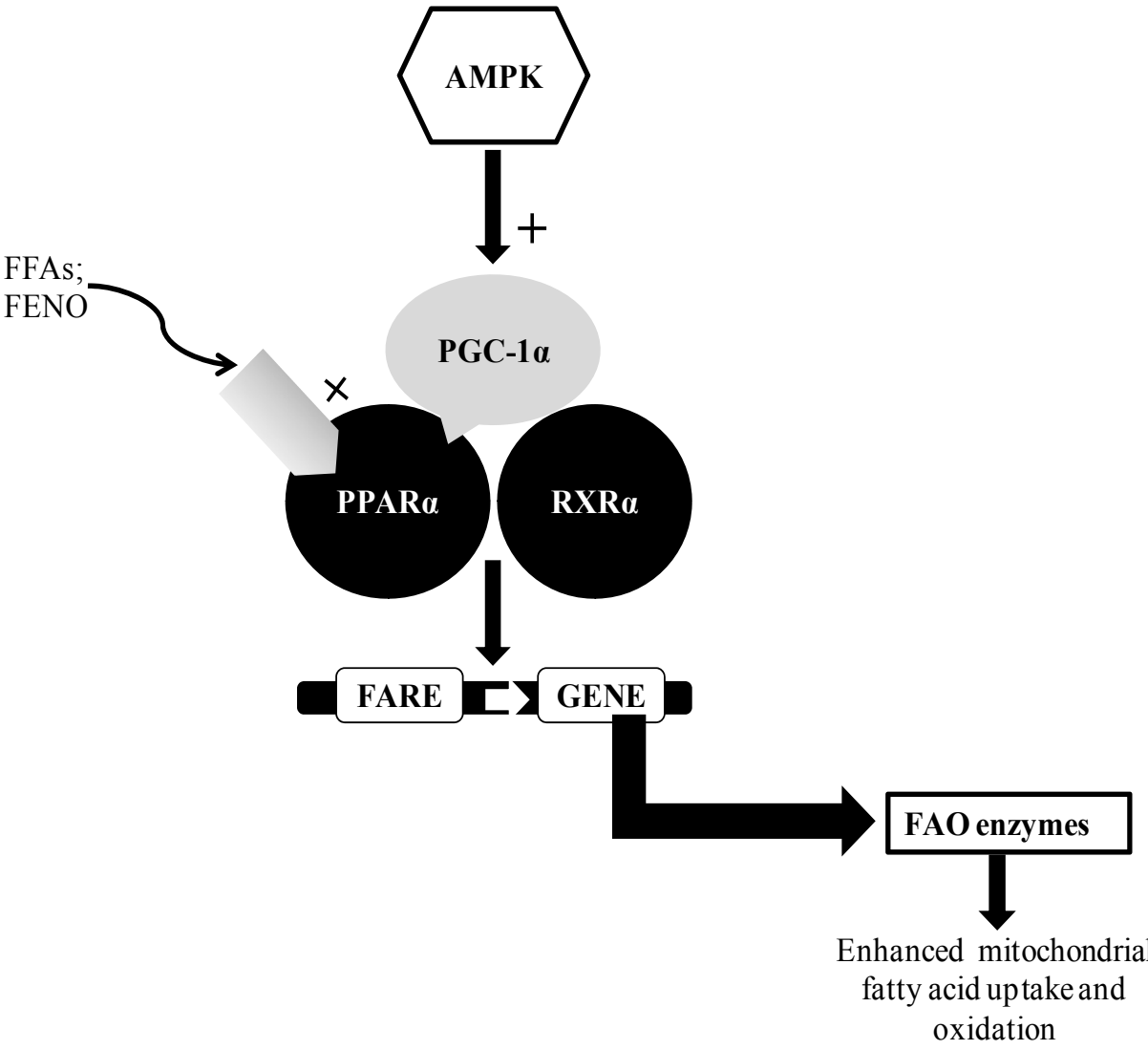

Figure 3. Transcriptional control of FAO. *FFAs indicates free fatty acids; FENO, fenofibrate; PGC-1α, peroxisome proliferator-activated receptor gamma coactivator-1 alpha; PPARα, peroxisome proliferator-activated receptor alpha; RXRα, retinoid X receptor alpha; FARE, fatty acid response element; FAO, fatty acid oxidation.* ***Figure adapted from Lehman and Kelly, 2002.***

Since PGC-1α also interacts with PPARα via ligand-reliant communications, PGC-1α allows changes in FAO to be closely matched with mitochondrial biogenesis (Vega et al 2000); see figure 3 for an illustration of the PPARα/PGC-1α interaction. For instance, under strenuous conditions such as exercise and hypertrophy, cardiac mitochondrial energy generation is elevated via increased PGC-1α expression (Lehman et al 2000). PGC-1α also increases mitochondrial transcription factor A (TFAM) and nuclear respiratory factor-1 (NRF-1) expressions via ligand-reliant communications; since TFAM is a transcription factor that controls mitochondrial DNA transcription and replication, PGC-1α increases mitochondrial biogenesis (Lehman et al 2000 and Wu et al 1999). In mice with decreased expression of TFAM, cardiomyopathy associated with decreased mitochondrial DNA (mtDNA) and respiratory chain dysfunction occurs (Hansson et al 2004). NRF-1 controls mitochondrial respiration by upregulating genes encoding subunits of ETC complexes I-IV (Vega et al 2000). NRF-1 also regulates transcription and replication of mtDNA via interactions with TFAM and PGC-1α (Kelly and Scarpulla, 2004 and Gopalakrishnan and Scarpulla, 1995). Upregulation of NRF-1 mRNA expression was linked to elevation of mitochondrial mass following electrical stimulation in neonatal cardiomyocytes, thus NRF-1 is also important for mitochondrial biogenesis (Xia et al 1997). Certainly, PGC-1α interacts with NRF-1 to induce mitochondrial biogenesis (Wu et al 1999); transcriptional control of mitochondrial structure, function and respiration by PPARα, PGC-1α, TFAM and NRF-1 are summarized in figure 4A and 4B.

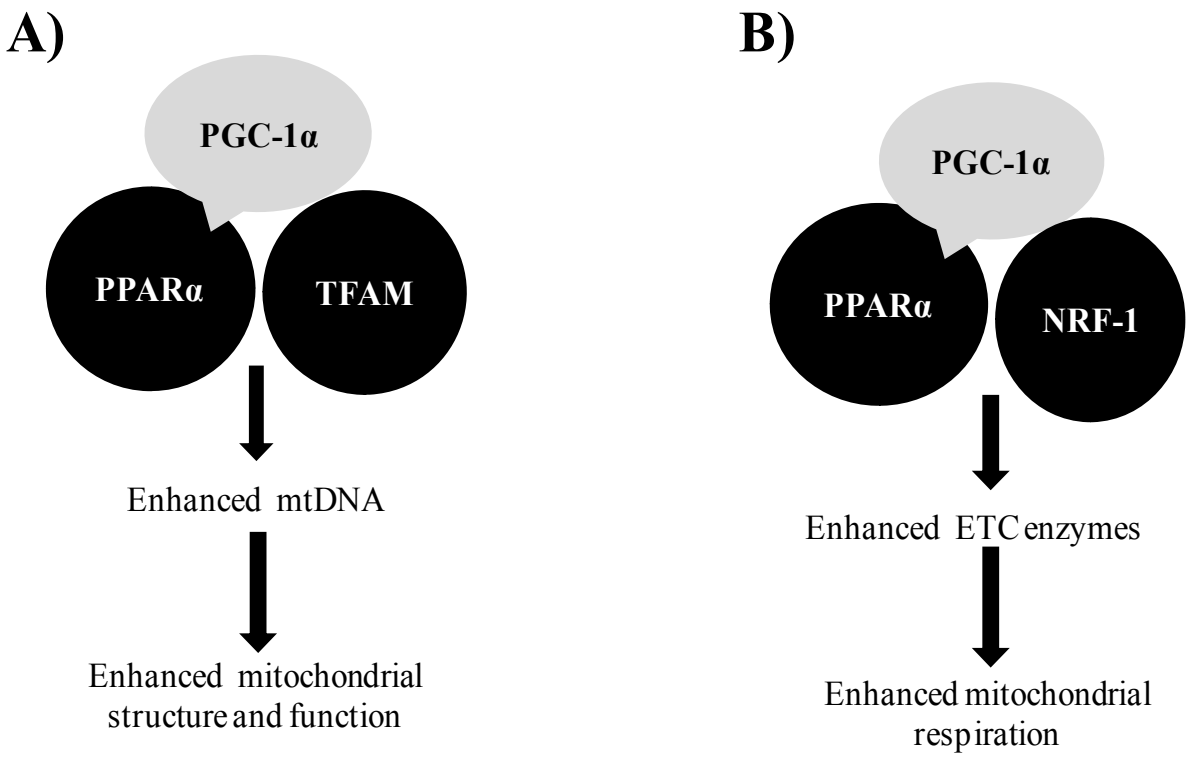

Figure 4. Transcriptional control of mitochondrial structure, function (A) and respiration (B). *PGC-1α, peroxisome proliferator-activated receptor gamma coactivator-1 alpha; PPARα, peroxisome proliferator-activated receptor alpha; ETC, electron transport chain; mtDNA, mitochondrial DNA.*

1.3. Cardiac metabolism in LVH and heart failure

Various animal models of cardiac hypertrophy and failure have shown that genes and proteins essential for FA transport, uptake and oxidation are downregulated (Akki et al 2008, Lei et al 2004, Osorio et al 2002, Rosenblatt-Velin et al 2001 and Taylor et al 2001). These studies suggest that during failure, the heart becomes more reliant on glucose metabolism to generate ATP. The pattern of gene expression seen in heart failure resembles that in the foetal heart since it favours glucose metabolism at the expense of decreased FA metabolism (Lehman and Kelly, 2002). While the change in substrate preference towards glucose metabolism reduces the cost of oxygen utilization and metabolic demand, energy generated from the oxidation of one glucose molecule is less than energy generated from one FA molecule (Van Bilsen et al 2009). A small reduction in FAO would consequently require a large increase in glucose metabolism in order to avert energy depletion. In line with this thinking, other studies have shown that sustained cardiac reduction of FAO causes progressive energy depletion since a concurrent increase in glucose oxidation is not sufficient as an alternative mechanism of energy generation (Neglia et al 2007 and Recchia et al 1998).

As explained earlier, PPARα plays a key role in the transcriptional control of genes responsible for FA transport, uptake and metabolism. It has been shown in experimental models of heart failure that downregulation of PPARα is linked to cardiac energy depletion (Finck and Kelly, 2002). Additionally, late stage pacing-induced heart failure is also characterized by downregulation of proteins involved in FA transport and oxidation such as CPT-1 and MCAD respectively (Lei et al 2004 and Osorio et al 2002). Downregulation of the mRNA expression of PPARα, MCAD, FABP and CPT-1 has been reported in the infarct model of heart failure at end-stage (Iemitsu et al 2002, Remondino et al 2000 and Ruderman et al 1999). Furthermore, human

end-stage heart failure is associated with downregulation in protein expression of both PPARα and CPT-1 (Karbowska et al 2003 and Depre et al 1998). These studies suggest that lowered energy production from FFAs as a direct result of PPARα downregulation contributes to cardiac hypertrophy and failure.

Low energetic capacity in heart failure may further be worsened by mitochondrial degeneration. For example, Schaper et al (1991) showed that mitochondrial number, size and structural arrangement are altered in heart failure. Mitochondrial defects have been associated with altered expression of genes such as TFAM and NRF-1, which are involved in maintenance of the structural integrity and biogenesis of mitochondria (Garnier et al 2003). The expressions of TFAM, NRF-1 and PGC-1α are reduced in some models of heart failure and these changes were associated with mitochondrial dysfunction (Javadov et al 2006; Barger and Kelly, 2000). Mitochondrial dysfunction has been established in late-stage heart failure (Murray et al 2008 and Bugger et al 2006). Reductions in mitochondrial oxygen consumption rate and activities of complex I-IV of the respiratory chain have been reported in some animal models of heart failure (Javadov et al 2006, Scheubel et al 2002, Ide et al 2001 and Sanbe et al 1995).

In addition to substrate switching from FAs to glucose, phosphocreatine (PCr) content is reportedly reduced in heart failure, which results in the lowering of PCr/ATP ratio (Kalsi et al 1999 and Shen et al 1999). Since PCr/ATP ratio is regarded as an indicator of energy reserve, cardiac energy reserves are therefore limited in heart failure. Various other studies have established that changes in metabolic state during cardiac hypertrophy and failure include a reduction in high-energy phosphates (Neubauer, 2007; van Bilsen et al 2004; Ingwall and Weiss, 2004).

It still remains controversial whether metabolic changeover from FFAs to glucose is beneficial or harmful to the heart. A generally held view is that in the short-term, at least during hypertrophy, relative reduction in availability of oxygen and ATP may require this shift in metabolism from FA to glucose since it would significantly lower the requirement for oxygen. Conversely, in addition to energy depletion, continued reliance on glucose metabolism and therefore decreased usage of FFAs may also induce cardiomyocyte lipotoxicity. Certainly, more studies are necessary to determine the beneficial or harmful interactions between myocardial and metabolic remodelling. At present, therapeutic interventions that lower PPARα activity in the hypertrophic heart could be beneficial for short-term myocardial function. However, maintenance of long-term myocardial function may require PPARα activation to prevent energy depletion and lipotoxicity. Other than preventing energy depletion and lipotoxicity, PPARα activation may also upregulate cardiac anti-inflammatory and anti-oxidant processes (Guellich et al 2007 and Delerive et al 2001). However, others have also suggested that reactivation of PPARα during LVH is deleterious (Young et al 2001). Therefore, the role of PPARα in LVH and heart failure requires further investigation.

1.4. Neurohormonal activation in heart failure

In heart failure, stimulation of β_1-adrenergic receptors has favourable effects in the early phases since it sustains cardiac output by increasing contraction and heart rate (Braunwald et al 2001). However, a sustained increase in concentration of catecholamines coincides with increases in the severity of heart failure; hence, others have suggested that catecholamines may play an important role in the progressive heart failure (Francis et al 1990). Further, activation of a pathway directly associated with the neurohormonal mechanism using isoproterenol in experimental studies

induces LV remodelling (Osadchii et al 2007, Badenhorst et al 2003 and Beltrami et al 1994). Isoproterenol is a β-adrenergic receptor agonist that can increase both myocardial contractility and heart rate. However, when administered chronically in low doses, isoproterenol causes progressive left ventricular remodelling characterized by structural and functional changes (Woodiwiss et al 2001 and Cohn et al 2000).

The neurohormonal hypothesis states that the main drivers of the progression of heart failure are endogenous neurohormones and cytokines that could be triggered by an acute insult to the heart (Parker, 1992). Activation of various neurohormones has been demonstrated in a clinical study of heart failure (Francis et al 1993). Once activated, neurohormones and cytokines mediate a series of events that induce a change in the structure of the myocardium (Francis and Carlyle, 1993; Pfeffer and Braunwald, 1990). Some of the events that are mediated by neurohormones and cytokines include loss of collagen, interstitial fibrosis, cardiomyocyte apoptosis, necrosis, inflammation and hypertrophy (Weber, 1997; Narula et al 1996 and Beltrami et al 1995). For example, increased angiotensin II, a neurohormone, causes upregulation of genes that stimulate cardiac hypertrophy (Larkin et al 2004). During progression of heart failure, increased angiotensin II induces a rise in the concentration of endothelin in plasma. Endothelin mediates myocardial fibrosis and can on its own initiate cardiomyocyte apoptosis (Braunwald, 2001). Consequently, endothelin contributes to LV remodelling and progression of heart failure. Pro-inflammatory cytokines such as tumor necrosis factor alpha, interleukin 1β and interleukin 6 have also been shown to be increased in heart failure and have been implicated in LV remodelling since they also contribute to myocardial fibrosis and cardiomyocyte apoptosis (Mann and Young, 1994; Yokohama et al 1993).

Prevention of neurohormonal activation has only worked partially in the treatment of clinical heart failure since heart failure remains one of the leading causes of death throughout the world (Ergin et al 2004, Roger et al 2004 and Juenger et al 2002). Currently, medical therapies used in heart failure such as angiotensin converting enzyme inhibitors, angiotensin II receptor antagonists, β-adrenergic receptor antagonists and aldosterone receptor antagonists target neurohormonal deactivation and have shown beneficial outcomes against some symptoms but have been unable to prevent the progression to heart failure (Tang and Francis, 2003; Sabbah et al 2000 and Bristow et al 1996). It is thus worth exploring other therapies that are not directly associated with the neurohormonal mechanism as possible therapies for heart failure or to supplement the therapies investigated in these studies.

Whether sympathetic nervous system (SNS) activation observed in heart failure contributes to metabolic dysfunction and worsened outcomes is still under investigation. SNS activation stimulates release of FFAs from adipocytes (Havel and Goldfien, 1959); SNS activation would therefore increase availability of plasma FFAs to the failing heart. Potentially, SNS activation may therefore induce metabolic dysfunction and lipotoxicity as a result of accumulation of FFAs.

Although SNS activation has long been identified in chronic heart failure, few studies have been done to investigate the role of sympathetic activation on cardiac metabolism. However, these studies have investigated the effect of acute, high dose isoproterenol administration on cardiac substrate metabolism and gene regulation (Heather et al 2009 and Yuan et al 2008). In Heather et al (2009), isoproterenol induced downregulation of fatty acid metabolism by reducing the expression of mitochondrial FAO enzymes (MCAD, citrate synthase, FAT/CD36 and FABP). In support, Yuan et al (2008) have reported isoproterenol-induced downregulation of PPARα,

MCAD and CPT-1. Still, the effects of chronic administration of low dose isoproterenol on cardiac metabolic gene profile are unknown.

The isoproterenol model represents mild heart failure that is characterized by myocardial damage as a result of myocyte death (Pearce, 1906). Another possible cause of heart failure following administration of a β-adrenergic receptor agonist has been suggested to be the diminished ability of mitochondria to recruit oxidative phosphorylation (Dhalla et al 1978). While the structural LV remodelling that occurs following chronic isoproterenol administration is well characterized, little is known about the contribution of metabolic and mitochondrial changes to LV structural and functional changes.

1.5. Hypothesis

We hypothesize that isoproterenol-induced cardiac changes will be accompanied by downregulation of genes essential for metabolic function such as PPARα, PGC-1α and AMPKα_2. We also predict that the administration of isoproterenol will induce mitochondrial dysfunction via downregulation of TFAM and NRF1. Fenofibrate, a PPARα agonist will prevent these genetic changes, thereby preserving metabolic state, mitochondrial function and cardiac function; the proposed mechanisms of fenofibrate-mediated cardioprotection are summarized in figure 5.

1.6. Study objectives

In this dissertation, the following objectives will be ascertained:

- Whether isoproterenol-induced cardiac remodelling is associated with downregulation of key metabolic genes such as peroxisome proliferator-activated receptor alpha (PPARα), AMP-activated protein kinase alpha 2 ($AMPK\alpha_2$) and PPARγ coactivator-1 alpha (PGC-1α).
- Whether isoproterenol induces mitochondrial pathology via downregulation of mitochondrial transcription factor (TFAM) and nuclear respiratory factor-1 (NRF-1) mRNA expressions.
- Whether fenofibrate, a PPARα agonist, prevents isoproterenol-induced cardiac structural and functional changes via metabolic remodelling and preservation of mitochondrial state.

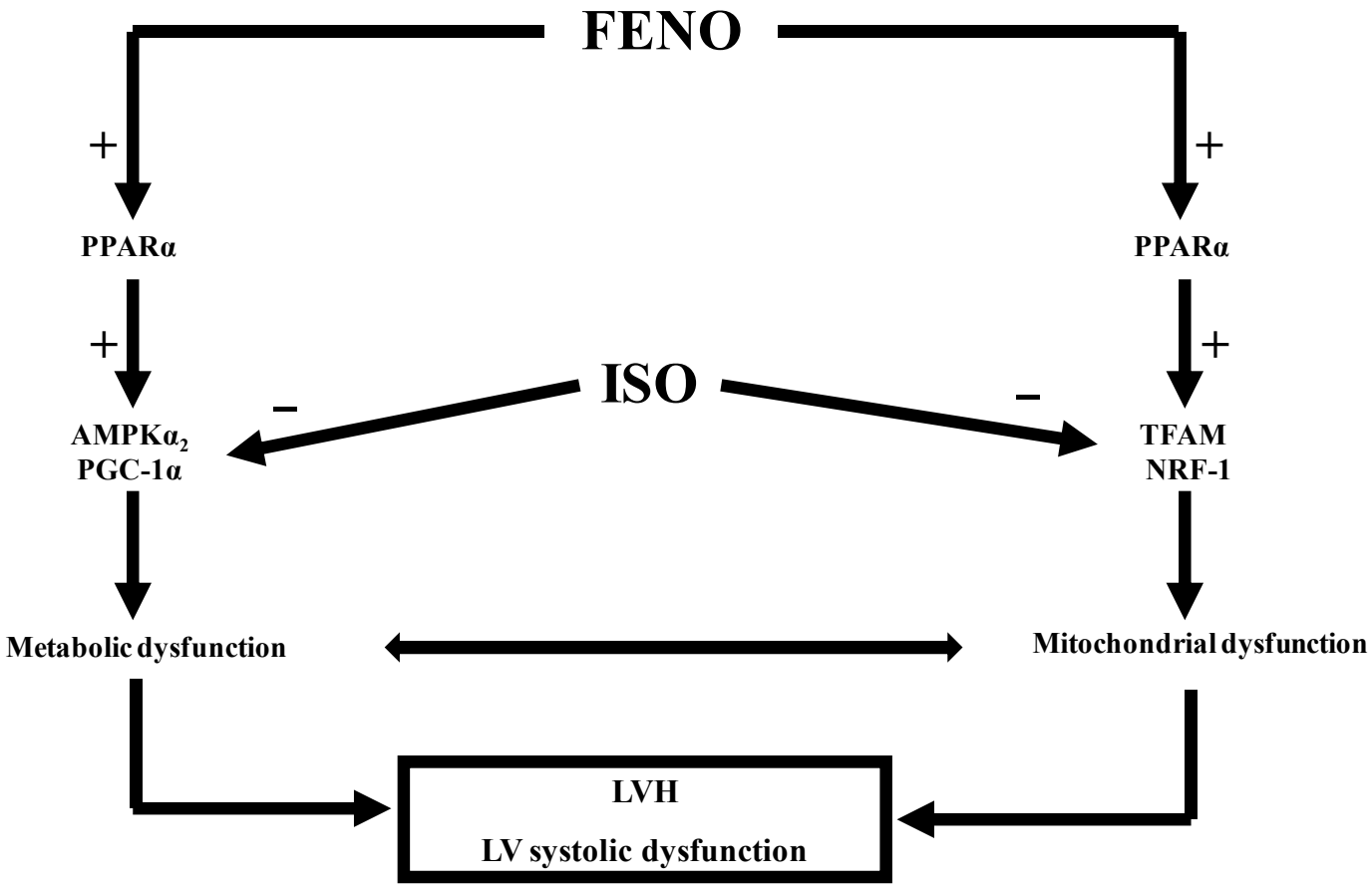

Figure 5. Hypothesis: Fenofibrate protects against isoproterenol-induced LVH and dysfunction via prevention of metabolic dysfunction and mitochondrial dysfunction. *ISO indicates isoproterenol; FENO, fenofibrate; PPARα, peroxisome proliferator-activated receptor alpha; AMPKα2, AMP-activated protein kinase alpha2; , PGC-1α, PPARγ coactivator-1 alpha; TFAM, mitochondrial transcription factor A; NRF-1, nuclear respiratory factor-1.*

2. MATERIALS AND METHODS

2.1. Materials

Isoproterenol hydrochloride (Sigma, USA); Fenofibrate (Sigma, USA); Gelatine (Davis Gelatine, Johannesburg, South Africa); brown sugar (Local supermarket); Bovril (Bovril, Unilever, Johannesburg, South Africa); Acuson Sequoia C-256 echocardiograph machine (Siemens Medical Division USA, Inc); Aquasonic 100 Ultrasound Transmission Gel (Parker Laboratories, USA); Ketamine (Bayer, Edms, Isando, South Africa); Xylazine, (Bayer, Edms, Isando, South Africa); Sabax Sodium Chloride (Saline), 0.9% (Adcock Ingram, South Africa); Free Fatty Acids, Half-micro test kit (Roche Diagnostics, Germany); ACCUTREND glucose strips, triglyceride strips and GCT meter (Roche Diagnostics, Germany); RNA later (Southern Cross Biotechnology, South Africa); Nucleospin RNA 4 kit (Macherey-Nagel, Germany); Reverse transcriptase kit (Roche Diagnostics, Germany); Synergy Brands (SYBR), Inc. Green Kit (Roche Diagnostics, Germany); 20µl light-cycler capillaries (Roche Diagnostics, Germany); light-cycler 4.0 PCR machine (Roche Diagnostics, Germany); light-cycler 4.0 software (Roche Diagnostics, Germany).

2.2. Methods

2.2.1. Ethical approval

Ethical approval for all experiments was obtained from the Animal Ethics Screening Committee of the University of the Witwatersrand (Clearance number: 2008/6/04).

2.2.2. Preparations

a) Isoproterenol preparation

5 mg of isoproterenol was weighed and dissolved in 50ml of saline to make up the stock solution. To achieve a final dose of $0.04mg.kg^{-1}.day^{-1}$, 0.12ml of the stock solution was injected to a 300g rat per day. The isoproterenol stock solution was prepared daily. In order to ensure that the correct dose was maintained, initial and weekly weights were obtained and the dose of isoproterenol was adjusted relative to rat body mass.

b) Gelatine cubes preparation

The vehicle solution was prepared by mixing 12g gelatine, 25.5g brown sugar; 7.5ml Bovril in 150ml of warm water as previously described (Kamerman et al 2004). Fenofibrate cubes were prepared by adding 750mg of fenofibrate into 50ml of the vehicle solution and mixed well to form a uniform fenofibrate suspension. The fenofibrate suspension was measured into 2ml syringes and the syringes were then refrigerated until the suspension solidified. A final dose of $100mg.kg^{-1}.day^{-1}$ was administered and the dose of fenofibrate was adjusted weekly relative to rat body mass.

c) Anaesthetic preparation

The anaesthetic solution was prepared by mixing 1ml of ketamine and 1ml of xylazine with 8ml of saline. For anaesthesia, the anaesthetic solution was injected intraperitoneally at doses of 75mg.kg^{-1} ketamine and 15mg.kg^{-1} xylazine. Echocardiography was performed 24hours after the last dose of isoproterenol. After echocardiography, each animal was euthanized by administration of an overdose of the anaesthetic (extra 1ml) and tissue was collected for further analysis.

2.2.3. Animal model and experimental protocol

The isoproterenol model of heart failure is well established and has been used in many studies of systolic chamber dysfunction (Norton et al 2002, Woodiwiss et al 2001 and Teerlink et al 1994). Briefly, in the isoproterenol model, daily administration of low dose (0.04 or 0.05mg.kg^{-1}.day^{-1}) isoproterenol for a 1month period or longer causes progressive ventricular remodelling that begins with cardiac hypertrophy and later, prominent cardiac pump dysfunction (Osadchii et al 2007 and Woodiwiss et al 2001). In the current study, the isoproterenol model of heart failure was used to investigate whether changes in metabolic substrates, metabolic gene regulation and mitochondrial structure contribute to left ventricular hypertrophy and dysfunction.

Eighty male Sprague-Dawley (SD) rats weighing 250-300g were obtained from the Central Animal Services of the University of the Witwatersrand. The rats were housed in individual cages and had access to food and clean drinking water. Sixteen rats were not included in the final analysis as they died from sudden cardiac arrest following isoproterenol injections. Therefore the study will be reported on sixty-four rats.

Rats were allocated into 4 different groups as follows: untreated control (CONTROL, n=16); fenofibrate (FENO, n=16), which received fenofibrate in gelatine cubes at a dose of 100mg.kg^{-1}.day^{-1}. Isoproterenol treated group (ISO, n=24), which received subcutaneous injections of isoproterenol at 0.04mg.kg^{-1}.day^{-1}. Lastly, in the ISO+FENO (n=24) group, rats were administered with both isoproterenol and fenofibrate as previously explained; the experimental design is summarized in figure 6. For consistency, daily ISO injections were performed in the late afternoon (16:00-18:00). The dose of fenofibrate was chosen because it has been used previously and shown to be non-toxic to rats (LeBrasseur et al 2007 and Morgan et al 2005).

2.2.4. Metabolic substrate measurements

Plasma concentrations of glucose, free fatty acids (FFAs) and triglycerides (TGs) have been shown to be altered in different stages of heart failure and are thought to play significant roles in metabolic gene changes associated with the development of heart failure (Taegtmeyer, 2002). To determine blood glucose and TG concentrations, rats were fasted for 16hours and blood was collected from tail veins. Briefly, blood glucose and TG concentrations were measured using glucose and triglycerides strips inserted into an ACCUTREND GCT meter. A small cut was made at the tip of the tail; one drop of blood was allowed on to the strip; the strip was inserted on to an ACCUTREND GCT meter and readings were obtained.

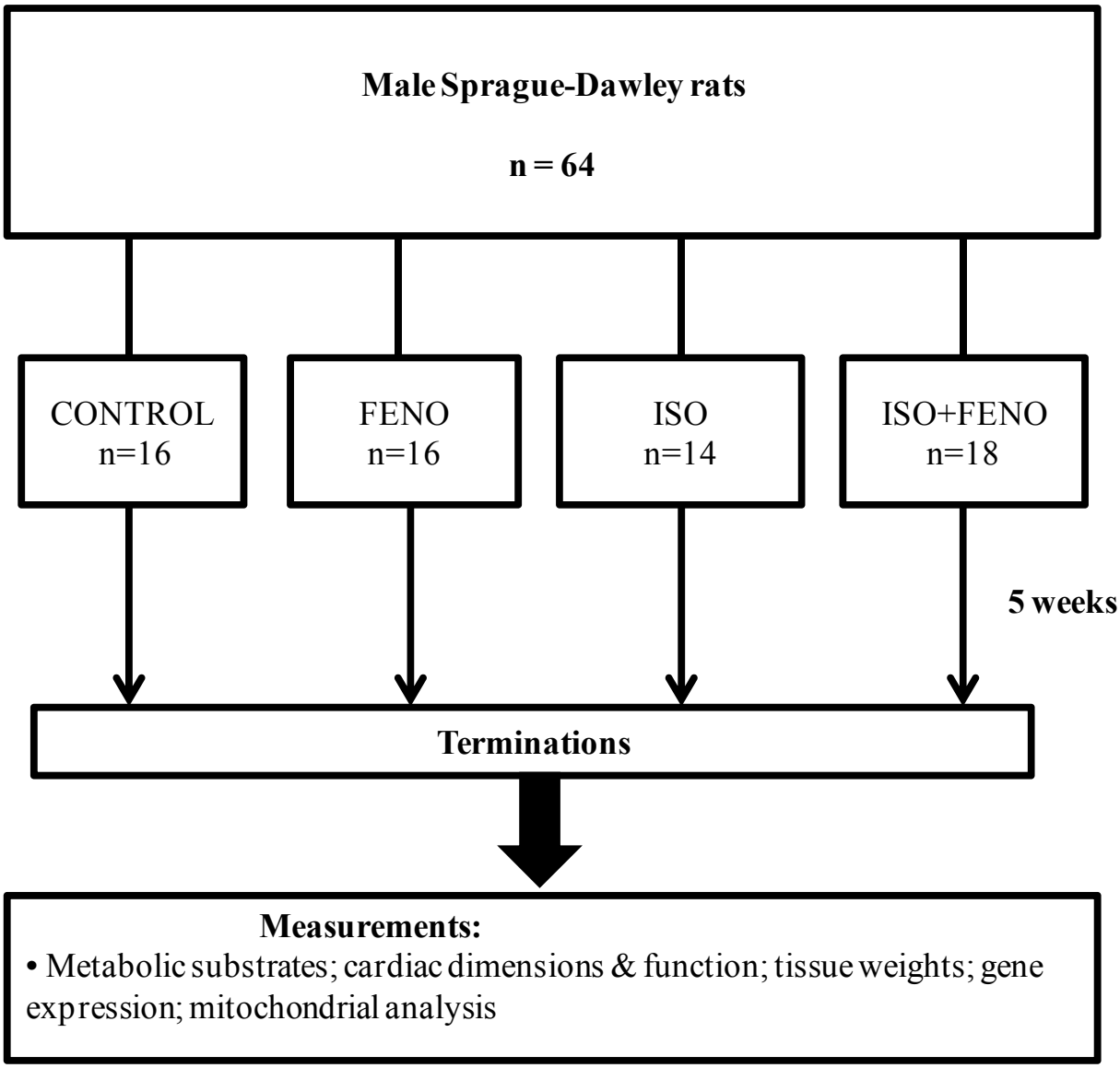

Figure 6. Experimental design. *CONTROL, indicates untreated group; FENO, the group that received fenofibrate; ISO, the group that was injected with isoproterenol; ISO+FENO, the group that was treated with both isoproterenol and fenofibrate.*

To determine plasma FFAs, 1ml of blood was collected immediately after the heart was excised; the blood was then centrifuged at 5000rpm for 10minutes and the supernatant (plasma) was collected, and then stored at +4°C. Plasma FFAs were measured colorimetrically using the Free Fatty Acids, Half-micro test kit according to the manufacturer's instructions.

To create a standard curve and ensure accurate measurement, a standard solution was prepared. To prepare the standard, 80ml of solution 1 (6g triton X-100 in 80ml double distilled water) was mixed with solution 2 (9mg palmitic acid dissolved in 6ml of warm ethanol, 40°C). Briefly, the working solutions were prepared in two reaction mixtures, reaction mixture A and B. Reagents were mixed in cuvettes by gentle swirling after closing the cuvettes with parafilm. The blank was prepared by mixing 1ml of reaction mix A with 0.05ml double distilled water and the mixture was warmed and kept at 25°C for ten minutes. 0.05ml N-ethyl-maleinimide-solution was then added into the cuvette and mixed. The absorbance of the solution (A_1) in the cuvette was then read. The reaction was started by adding 0.05ml of reaction mix B to the cuvette and mixed. The absorbance of the solution (A_2) was read after incubation for 15minutes at 25 °C. To prepare the sample, 0.05ml of the sample was mixed with reaction mix A, instead of double distilled water and the same protocol as the blank preparation was followed. The concentration of plasma FFAs was calculated using this formula:

$C = (V/ e \times d \times v) \times \Delta A [\Delta A_S - \Delta A_b]$, where

C = concentration of plasma FFAs

V = final volume (ml)

v = sample volume (ml)

d = light path (cm)

e = absorption coefficient of the dye at 546 nm

ΔA_S = the absorbance difference of the sample

ΔA_b = the absorbance difference of the blank

2.2.5. Echocardiography

Echocardiography was used to determine cardiac remodelling and function as previously explained (Osadchii et al 2005, Norton et al 2002 and Woodiwiss et al 2001). Following anaesthesia, rats were shaved on the chest and placed in a prone position. Echocardiographic measurements were taken approximately 15minutes after an anaesthetic dose was administered. In order to measure cardiac dimensions, ultrasound transmission gel was spread around the probe. The probe was placed on the transthoracic region of the rat. Three investigator-blinded measurements of LV dimensions were then obtained using a 7.5 MHz transducer and Hewlett-Packard Sonos 2000 sector scanner and software present on the ultrasonograph. The cardiac dimensions that were measured included left ventricular end-diastolic diameter (LVEDD), left ventricular end-systolic diameter (LVESD), left ventricular end-diastolic posterior wall thickness (LVED PWT) and left ventricular end-systolic posterior wall thickness (LVES PWT). Cardiac dimensions were measured in centimetres and determined according to the American Society for Echocardiography's leading edge method (Sahn et al 1978). To determine LV chamber and myocardial systolic function, percentages of endocardial fractional shortening (FS_{end}) and

midwall fractional shortening (FS_{mid}) were determined using the cardiac dimensions as previously explained (Norton et al 2002 and Woodiwiss et al 2001) as follows:

Formulae for calculating FSend and FSmid

FS_{end} = LVEDD – LVESD/LVEDD x 100

FS_{mid} = ((LVEDD + LVED PWT) – (LVESD + LVES PWT))/LVEDD+ LVED PWT x 100

(The steps followed to determine LV function are summarized in figure 7).

2.2.6. Tissue measurements

The heart was excised from each rat and weighed, after which the left ventricle was separated from the right ventricle and septum to determine left ventricular (LVM) and right ventricular (RVM) mass. The left tibia was also removed from each rat and its length measured in cm using a ruler in order to determine tibial length (TL). The ratio of heart mass-to-tibial length was used to indicate the degree of cardiac hypertrophy. Since tibial length of rats changes minimally during growth compared to body mass (Berg and Harmison, 1958), ratio of heart mass-tibial length is a more accurate indicator of relative heart mass than heart mass-body mass ratios. Further, using heart mass-body mass ratios would presume that heart mass changes in proportion with body mass under normal conditions.

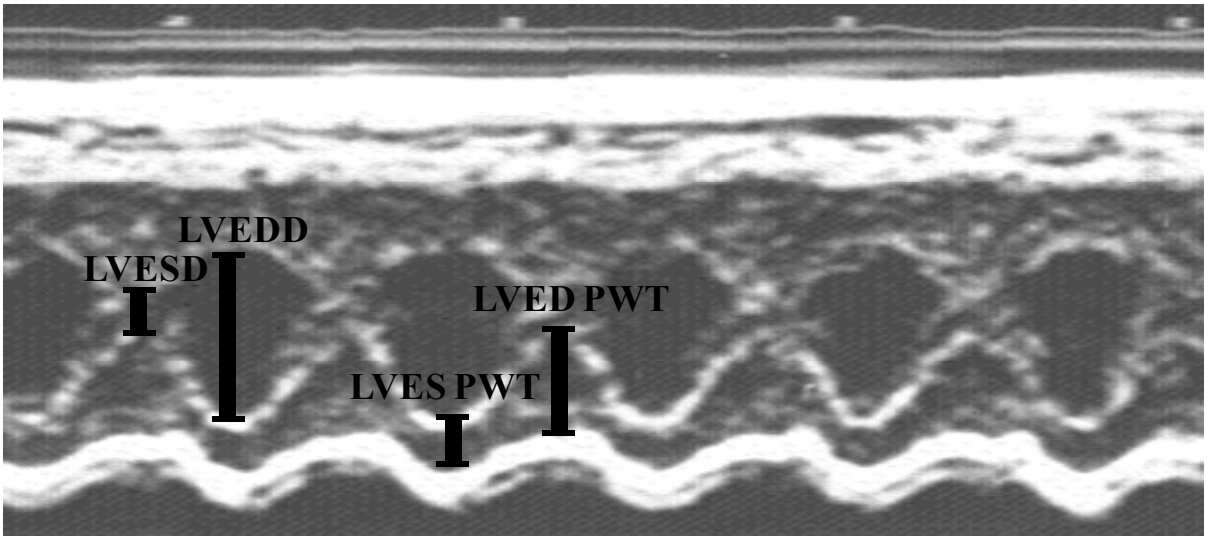

Endocardial Fractional Shortening → **Chamber function**

Midwall Fractional Shortening → **Myocardial function**

Figure 7. Determination of cardiac dimensions and function using echocardiography. *FS_{end} indicates endocardial fractional shortening; $FS_{mid,}$ midwall fractional shortening; LVEDD, left ventricular end-diastolic diameter; LVESD, left ventricular systolic diameter.*

Formulae for calculating relative heart mass

Relative total heart mass = HM/TL

Relative left ventricular mass = LVM/TL

Relative right ventricular mass = RVM/TL

2.2.7. Messenger RNA extraction (mRNA), complementary DNA synthesis and quantitative real-time polymerase-chain reaction (RT-PCR)

a) mRNA extraction

Transcript levels of PGC-1α, PPARα, NRF-1, TFAM and AMPKα_2 were measured using real-time polymerase chain reaction. Total RNA was isolated from LV tissue (approx. 0.60g) that was preserved in 1500µl RNA later solution and stored in a -20°C freezer for subsequent analysis. Briefly, 50mg of stored LV tissue was cut and preserved in 100µl RNA later solution before it was homogenised by freezing the sample in liquid N_2 and grinding using a pestle and mortar. Cell lysis of ground tissue was performed by adding 350µl lysis buffer RA1 and 3.5µl β-mercaptoethanol in a PCR tube, followed by 5minutes vortexing. The lysed tissue mixture was then applied to a Nucleospin® Filter Unit and centrifuged for 1 minute at 11,000xg. The Nucleospin® Filter Unit was discarded and 350µl of 70% ethanol was added to the homogenised lysate and mixed by pipetting up and down. The lysate was loaded to a Nucleospin® RNA II column placed in a 2ml collecting tube and centrifuged for 30 minutes at 11,000xg. The column was then placed in a new collecting tube. To desalt the silica membrane, 350µl membrane desalting buffer was added and the column was centrifuged 1 minute at 11,000xg to completely

dry the membrane. To digest DNA, a DNase reaction mixture was prepared by mixing 10µl reconstituted rDNase with 90µl reaction buffer for rDNase for each isolation. 95µl of DNase reaction mixture was directly added onto the centre of the silica membrane of the column and incubated at room temperature for 15minutes. To wash and dry the membrane, 200µl buffer RA2, followed by 600µl buffer RA3 and 250µl buffer RA2 were applied to the Nucleospin® RNA II column, and then centrifuged at 11,000xg until the buffer was cleared off the column on each occassion. RNA was eluted in 60µl RNase-free water and the column centrifuged for 1minute at 11,000xg. Eluted RNA was stored in a -80°C freezer for subsequent analysis.

b) cDNA synthesis and quantitative RT-PCR

Complementary DNA was synthesized from the RNA using a reverse transcriptase kit. Briefly, 2µl of PCR grade water was mixed with 1µl anchored-oligo (dT) 18 primer and was added to 10µl mRNA in RNase-, DNase-free PCR tube. The tube was incubated at 65°C for ten minutes and then immediately placed on ice. Transcriptor RT reaction buffer (4µl); protector RNase inhibitor (0.5µl); deoxynucleotide (2µl) and transcriptor reverse transcriptase (0.5µl) were added into the PCR tube and mixed well by pipetting up and down. The tube was spun briefly in a microfuge and then incubated at 55°C for 30 minutes and at 85°C for 5 minutes. The tube with cDNA was immediately placed on ice and stored in a -20°C freezer. 2µl of cDNA was added to a solution made up of PCR grade water (12µl); forward primer (1µl); reverse primer (1µl) and master mix (4µl, prepared from SYBR Green Kit) in a 20µl light-cycler capillary. Transcriptional targets such as PGC-1α, PPARα, NRF-1, TFAM and AMPKα_2 were amplified (in duplicates) using appropriate primers on a Synergy Brands (SYBR), Inc. Green Kit and a light-cycler PCR

machine according to the manufacturer's instructions (see table 1 for primer sequences). RT-PCR conditions were chosen following optimization experiments to determine the correct reaction conditions. The target transcripts were analyzed using the light-cycler 4.0 software. Levels of mRNA were quantified relative to expression of constitutively expressed gene, glyceraldehyde-3-phosphate dehydrogenase (GAPDH), which was used as an internal standard.

2.2.8. Electron transmission microscopy

Electron microscopy was used to determine mitochondrial degeneration and number. LV tissue, cut longitudinally from the base to the apex into small pieces of 1mm thick, was fixed in 2.5% gluteraldehyde and 2% paraformaldehyde in phosphate buffered saline, PBS pH 7.3, and then postfixed in 1% osmium tetroxide. For dehydration, specimens were immersed sequentially in 50%, 70%, 80%, 95% and 100% ethanol and embedded in fresh resin mix (5.62g Araldite, 7.75 Epon 812, 15g DDSA and 0.71g DMP30). After incubation for 48 hours at 60°C, the specimens were cut into ultra thin tissue sections. For staining, the grids were treated with uranyl acetate (saturated solution in methanol), followed by lead citrate (1% aqueous solution + 4% conc NaOH (i.e. 1ml NaOH/25ml 1% lead citrate). Specimens were allowed to dry and examined with a transmission microscope at 5000x magnification to determine mitochondrial arrangement and at 40000x magnification to assess the integrity of cristae. Micrographs were also examined for any other cardiac muscle and mitochondrial structural abnormalities at both 5000x and 40000x magnifications. Micrographs from CONTROL samples were first examined to measure degree of changes in samples from other groups against CONTROL. For each sample, four-to-six micrographs were photographed at 5000x magnification from four-to-six specimens for use in

Table 1. Primer sequences that were used in RT-PCR experiments

Gene	Sense	Sequence
i) AMPKα_2	Forward	CAG GGA CTG CTA CTC CAC AGA GAC
	Reverse	CTT GAG CCT CAG CAT CTG AA
ii) PPARα	Forward	TAG ATC CTC AAG ATC CTG TTA CTA TTA
	Reverse	GCC TTT CGT GCT CAT TGG
iii) PGC-1α	Forward	ATC ACC CGA GAG TTC CTA AA
	Reverse	CCG ATC TCC ACA GCA AAT TAT
iv) NRF-1	Forward	CAT TAG ATG AAT ATA CGA CAC GAG T
	Reverse	CTC CAG GTC TTC CAG GAT
v) TFAM	Forward	CAT ACC CTC GCC TGT CA
	Reverse	ATC AGT TCT GAA ACT TTT GCA T
vi) GAPDH	Forward	ATG CCA TCA CTG CCA CCC
	Reverse	GCC TGC TTC ACC ACC TTC TT

AMPKα_2 indicates AMP-activated protein kinase alpha 2; PPAR, peroxisome proliferator-activated receptor alpha; PGC-1α, peroxisome proliferator-activated receptor gamma coactivator-1alpha; NRF-1, nuclear respiratory factor-1; TFAM, mitochondrial transcription factor A; GAPDH, glyceraldehyde-3-phosphate dehydrogenase.

quantification. The area occupied by mitochondria was determined relative to the total area of the micrograph.

2.2.9. Statistical analysis

We used a one-way analysis of variance (ANOVA) followed by Tukey's post-hoc test to compare differences between the groups. Pearson's product-moment linear correlations were also performed to determine associations between metabolic gene regulation and cardiac function. Values are represented as means ± SEM and a $p<0.05$ was considered significant.

3. RESULTS

3.1. Body mass, visceral fat mass and tibial length

Body mass, visceral fat mass and tibial lengths are shown in table 2. There were no significant differences in body mass (CONTROL, 470.50±9.18g; FENO, 482.50±14.59g; ISO, 475.14±16.38g; ISO+FENO, 463.75±16.61g; NS), visceral fat mass (CONTROL, 13.94±1.00g; FENO, 14.26±1.77g; ISO, 11.56±1.30g; ISO+FENO, 10.49±1.13g; NS) and percentage body mass gain (CONTROL, 54.21±3.58%; FENO, 58.92±5.81%; ISO, 56.19±8.16%; ISO+FENO, 55.56±10.02%; NS) among the groups following 5 weeks of isoproterenol and fenofibrate administration. Thus, both isoproterenol and/or fenofibrate treatments did not affect body mass. There were also no significant differences in tibial length among the groups (CONTROL, 4.54±0.08cm; FENO, 4.74±0.08cm; ISO, 4.66±0.04cm; ISO+FENO, 4.63±0.05cm; NS), therefore administration of isoproterenol and fenofibrate did not affect growth.

3.2. Fenofibrate prevents isoproterenol-induced lowering of blood triglycerides

To determine metabolic substrate changes, fasted blood glucose, plasma free-fatty acids (FFAs) and blood triglycerides (TGs) concentrations were measured; the results obtained are shown in table 3.

Isoproterenol administration had no effect on fasted blood glucose and plasma FFAs concentrations (CONTROL, 7.17±0.23mmol/l vs ISO, 7.38±0.26mmol/l; NS and CONTROL, 0.50±0.06mmol/l vs. ISO, 0.54±0.08mmol/l, NS; respectively).

Table 2. Body mass, visceral fat mass and tibial length among all groups

	CONTROL	FENO	ISO	ISO+FENO
Body mass, g	470.50±9.18	482.50±14.59	475.14±16.38	463.75±16.61
Body mass gain, %	54.21±3.58	58.92±5.81	56.19±8.16	55.66±10.02
Visceral fat mass, g	13.94±1.00	14.26 ±1.77	11.56±1.30	10.49±1.13
Tibial length, cm	4.54±0.08	4.74±0.08	4.66±0.04	4.63±0.05
VFM/BM, mg/g	2.96±0.20	2.95±0.33	2.40±0.21	2.23±0.17
BM/TL, g/cm	3.07±0.22	3.01±0.37	2.49±0.28	2.10±0.21

Measurements were taken on the day of the termination following 5 weeks of Isoproterenol and fenofibrate treatments. VFM indicates visceral fat mass; BM, total body mass; TL, tibial length. Values are represented as means±SEM, n = 8-12.

However, blood TG concentrations were significantly decreased following isoproterenol administration (CONTROL, 1.86±0.12mmol/l vs. ISO 1.38±0.08 mmol/l; $p<0.05$).

Fenofibrate administration alone did not result in any significant differences in blood glucose, plasma FFAs and blood TG concentrations (7.00±0.35mmol/l; 0.50±0.07mmol/l and 1.64±0.12mmol/l, respectively, NS vs CONTROL). Interestingly, co-administration of isoproterenol with fenofibrate also did not have any effect on blood glucose concentration (ISO+FENO, 7.15±0.21mmol/l, NS vs CONTROL) and plasma FFAs (ISO+FENO, 0.48±0.06mmol/l, NS vs CONTROL) concentrations but prevented isoproterenol-induced decrease in TG concentrations (ISO+FENO 1.66±0.14mmol/l, NS vs CONTROL) although there was no significant difference in TG concentrations between ISO and ISO+FENO groups (NS vs ISO. Therefore, fenofibrate prevented isoproterenol-induced decrease in blood TG concentration.

3.3. Fenofibrate delays the onset of isoproterenol-induced left ventricular hypertrophy

Total heart mass (HM), left ventricular mass (LVM), right ventricular mass (RVM), tibial length (TL) were measured on the day of termination. Heart mass-to-tibial length (HM/TL), left ventricular mass-to-tibial length (LVM/TL) and right ventricular mass-to-tibial length (RVM/TL) ratios were then calculated to determine the magnitude of cardiac hypertrophy; the results obtained are shown in table 4.

Following 5 weeks of isoproterenol administration, significant increases in absolute HM (CONTROL, 1.17±0.03g vs. ISO, 1.33±0.04g; $p<0.05$), absolute LVM (CONTROL, 0.83±0.0.02g vs. ISO, 0.98±0.03g; $p<0.05$) and LVM/TL (CONTROL, 18.43±0.47 vs. ISO, 21.19±0.59; $p<0.05$) were observed in the ISO group compared to CONTROL group.

Table 3. Fenofibrate prevents isoproterenol-induced lowering of blood triglycerides

	CONTROL	FENO	ISO	ISO+FENO
Glucose, mmol/l	7.17±0.23	7.00±0.35	7.38±0.26	7.15±0.21
Free fatty acids, mmol/l	0.50±0.06	0.50±0.07	0.54±0.08	0.48±0.06
Triglycerides, mmol/l	1.86±0.12	1.64±0.12	1.38±0.08*	1.66±0.14

*Fasted metabolic substrate measurements were taken following 5 weeks of isoproterenol and/or fenofibrate treatments. *p<0.05 vs. CONTROL. Values are represented as mean±SEM, n = 6-8.*

However, there were no significant differences in absolute RVM (CONTROL, 0.31±0.01g vs. ISO, 0.35±0.0.02g; NS) and RVM/TL (CONTROL, 6.93±0.26 vs. ISO, 7.58±0.43; NS) between control and ISO groups. These data further suggest that isoproterenol induces left ventricular hypertrophy; however, isoproterenol has no effect on the right ventricle. Following administration of fenofibrate alone, there were no significant differences in absolute HM (CONTROL, 1.17±0.03g vs. FENO, 1.20±0.04g; NS). Also, absolute LVM (CONTROL, 0.83±0.0.02g vs. FENO, 0.88±0.02g; NS) and LVM/TL (CONTROL, 18.43±0.47 vs. FENO, 18.84±0.47; NS) and RVM/TL (CONTROL, 6.93±0.26 vs. FENO, 7.15±0.43; NS) ratios between the FENO and CONTROL groups were unchanged. Interestingly, fenofibrate prevented the onset of isoproterenol-induced left ventricular hypertrophy; LVM (ISO, 0.98±0.03g vs. ISO+FENO, 0.90±0.0.02g; $p<0.05$) between the ISO compared to ISO+FENO group. Furthermore, there was no significant difference in absolute HM (CONTROL, 1.17±0.03g vs. ISO+FENO, 1.23±0.03g; NS), absolute LVM (CONTROL, 0.83±0.0.02g vs. ISO+FENO, 0.90±0.02g; NS) and LVM/TL (CONTROL, 18.43±0.47 vs. ISO+FENO, 19.70±0.59; NS) between CONTROL compared to ISO+FENO.

3.4. Fenofibrate prevents isoproterenol-induced LV systolic chamber dysfunction

Cardiac dimensions such as left ventricular end diastolic diameter (LVEDD), left ventricular end systolic diameter (LVESD), left ventricular end diastolic posterior wall thickness (LVED PWT) and left ventricular end systolic posterior wall thickness (LVES PWT) were obtained using echocardiography and used to assess left ventricular structure and function; the cardiac dimensions obtained are shown in figures 8 and 9.

Table 4. Fenofibrate prevents the onset of isoproterenol-induced LV hypertrophy

	CONTROL	FENO	ISO	ISO+FENO
HM, g	1.17±0.03	1.20±0.04$^{\#}$	1.33±0.04*	1.23±0.03
LVM, g	0.83±0.02	0.88±0.02$^{\#}$	0.98±0.03*	0.90±0.02$^{\#}$
RVM, g	0.31±0.01	0.33±0.02	0.35±0.02	0.35±0.02
LVM/TL × 10^2	18.43±0.47	18.84±0.47$^{\#}$	21.19±0.59*	19.70±0.59
RVM/TL × 10^2	6.93±0.26	7.15±0.43	7.58±0.4	7.62±0.42

*Measurements were taken on the day of the termination following 5 weeks of Isoproterenol and/or fenofibrate treatments. HM indicates total heart mass; LVM, left ventricular mass; RVM, right ventricular mass; VM, visceral fat mass; BM, total body mass; TL, tibial length. *p<0.05 vs. CONTROL; $^{\#}$p<0.05 vs. ISO. Values are represented as means±SEM, n = 8-12.*

There were no significant differences in LVEDD (figure 8A) (CONTROL, 7.31±0.20mm vs. ISO 7.52±0.32mm, (NS vs. Control), LVESD (figure 9A) (CONTROL, 3.36±0.17mm vs. ISO, 4.22±0.25mm; NS vs. Control), LVED PWT (figure 8B) (CONTROL, 1.76±0.07mm vs. ISO, 1.93±0.13mm; NS vs. Control) and LVES PWT (figure 9B) (CONTROL, 2.95±0.08mm vs. ISO, 2.68±0.10mm; NS) between control and ISO groups.

Also, administration of fenofibrate alone did not result in any significant differences in LVEDD (figure 8A) (CONTROL, 7.31±0.20mm vs. FENO, 7.10±0.30mm; NS), LVESD (figure 9A) (CONTROL, 3.36±0.17mm vs. FENO, 3.24±0.28mm; NS) LVED PWT (figure 8B) (CONTROL, 1.76±0.07mm vs. FENO, 2.05±0.10mm; NS) or LVES PWT (CONTROL, 2.95±0.08mm vs. FENO 3.13±0.11mm; NS).

Interestingly, LVES PWT was significantly reduced in the ISO group compared to the FENO group (FENO, 3.13±0.11mm vs. ISO, 2.68±0.09mm; $p<0.05$). However, there was no significant difference in LVES PWT between ISO compared to ISO+FENO group (ISO, 2.68±0.09mm vs. ISO+FENO, 2.97±0.07mm; NS).

Endocardial fractional shortening (FS_{end}) and midwall fractional shortening (FS_{mid}) are shown in figure 10A and B. FS_{end} was significantly decreased in ISO compared to CONTROL group (CONTROL, 54.2±1.2% vs. ISO, 44.0±2.1%; $p<0.05$). Fenofibrate treatment did not induce any significant changes in FS_{end} (CONTROL, 54.2±1.2% vs. FENO, 54.8±2.5%; NS and CONTROL, 54.2±1.2% vs. ISO+FENO, 55.1±3.0%; NS). However, FS_{end} was also significantly decreased in the ISO compared to FENO group (FENO, 54.8±2.5% vs ISO, 44.0±2.1%; $p<0.05$) and ISO+FENO group (ISO, 44.0±2.1% vs. ISO+FENO, 55.1±3.0%; $p<0.05$). Fenofibrate thus prevented isoproterenol-induced reduction in cardiac chamber function.

There was no significant difference in FS_{mid} between control and isoproterenol groups (CONTROL, 30.5±1.1% vs. ISO, 26.9±1.3%; NS). There were also no changes in FS_{mid} following fenofibrate treatment (CONTROL, 30.5±1.1% vs. FENO, 30.4±1.6%; NS and CONTROL, 30.5±1.1% vs. ISO+FENO, 32.0±1.5%; NS).

3.5. Cardiac mRNA expression of metabolic regulation genes

Following five weeks of fenofibrate and/or isoproterenol administration, transcript levels of genes involved in metabolic regulation were measured in cardiac left ventricular tissue using RT-PCR.

3.5.1. Increased AMPKα_2 gene expression following co-administration of isoproterenol and fenofibrate

AMPKα_2 mRNA expression was measured to determine effects of isoproterenol and/or fenofibrate on cardiac metabolic demand; the results are shown in figure 11. There was no significant difference in cardiac AMPKα_2 mRNA expression in the FENO compared to CONTROL group (CONTROL, 0.83±0.17 vs. FENO, 0.81±0.18; NS). There was also no significant difference in cardiac AMPKα_2 mRNA expression in the ISO compared to CONTROL group (CONTROL, 0.83±0.17 vs. ISO, 0.31±0.07; NS). The ISO+FENO group had significantly higher cardiac AMPKα_2 mRNA expression compared to CONTROL (CONTROL, 0.83±0.17 vs. ISO+FENO, 2.18±0.70; $p<0.05$), FENO (FENO, 0.81±0.18 vs. ISO+FENO, 2.18±0.70; $p<0.05$) and ISO (ISO, 0.31±0.07 vs. ISO+FENO, 2.18±0.70; $p<0.05$), respectively. These results

suggest that administration of isoproterenol or fenofibrate alone does not regulate AMPKα_2 mRNA expression, however, simultaneous administration synergistically upregulates mRNA AMPKα_2 expression.

3.5.2. Downregulation of PPARα and PGC-1α gene expressions following co-administration of isoproterenol and fenofibrate

PPARα and PGC-1α mRNA expressions were measured since both genes are key regulators of mitochondrial FAO; the results are shown in figure 12A and B. Isoproterenol or fenofibrate administration alone did not have any effect on the cardiac gene expression of PPARα (CONTROL, 1.13±0.16 vs. FENO, 0.93±0.17; NS and CONTROL, 1.13±0.16 vs. ISO, 0.77±0.07; NS) and PGC-1α (CONTROL, 0.50±0.11 vs. FENO, 0.47±0.08; NS and CONTROL, 0.50±0.11 vs. ISO, 0.34±0.03; NS). Interestingly, co-administration of isoproterenol and fenofibrate significantly lowered cardiac mRNA expressions of PPARα (CONTROL, 1.13±0.16 vs. ISO+FENO, 0.52±0.05; $p<0.05$) and PGC-1α (CONTROL, 0.50±0.11 vs. ISO+FENO, 0.24±0.04, $p<0.05$). There was also a significant difference in cardiac PGC-1α mRNA expression between FENO compared to ISO+FENO (FENO, 0.47±0.08 vs. ISO+FENO, 0.24±0.04; $p<0.05$) while there was no significant difference in cardiac PPARα mRNA expression between FENO compared to ISO+FENO (FENO, 0.93±0.17 vs. ISO+FENO, 0.52±0.05; NS). Collectively, these results suggest that co-administration of isoproterenol and fenofibrate downregulates the mRNA expressions of PPARα and PGC-1α.

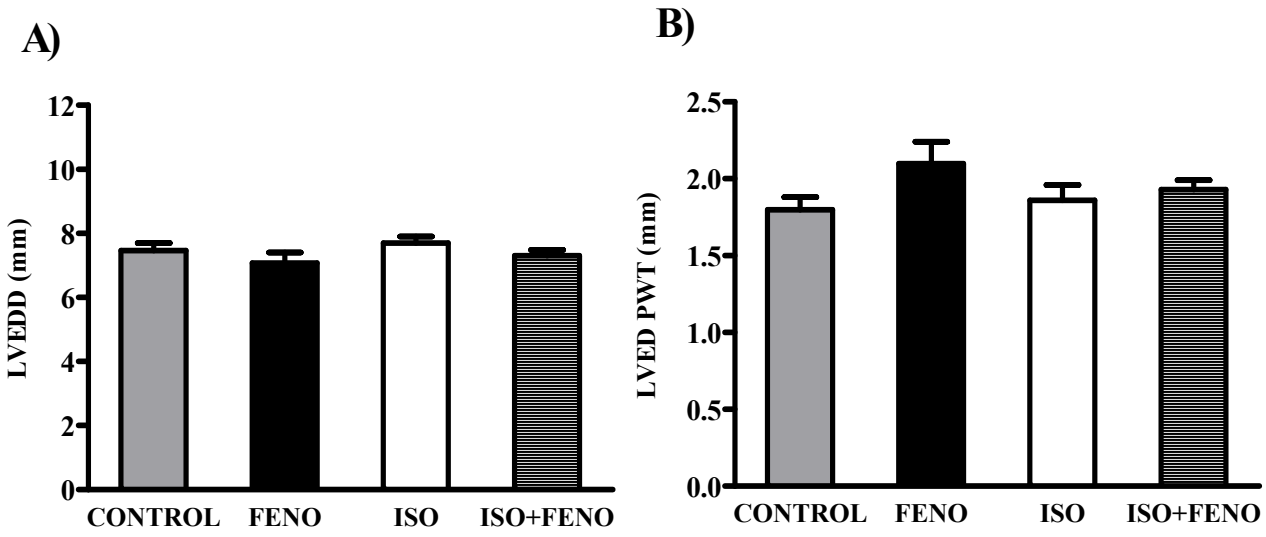

Figure 8. Cardiac diastolic dimensions as determined by echocardiography in rats. *Echocardiography was performed following five weeks of isoproterenol and fenofibrate administration in rats to determine cardiac dimensions. A) Left ventricular end systolic diameter (LVEDD); B) End systolic posterior wall thickness (LVED PWT). Between-group differences were tested using a one-way ANOVA. n=6-8. Values are means±SEM.*

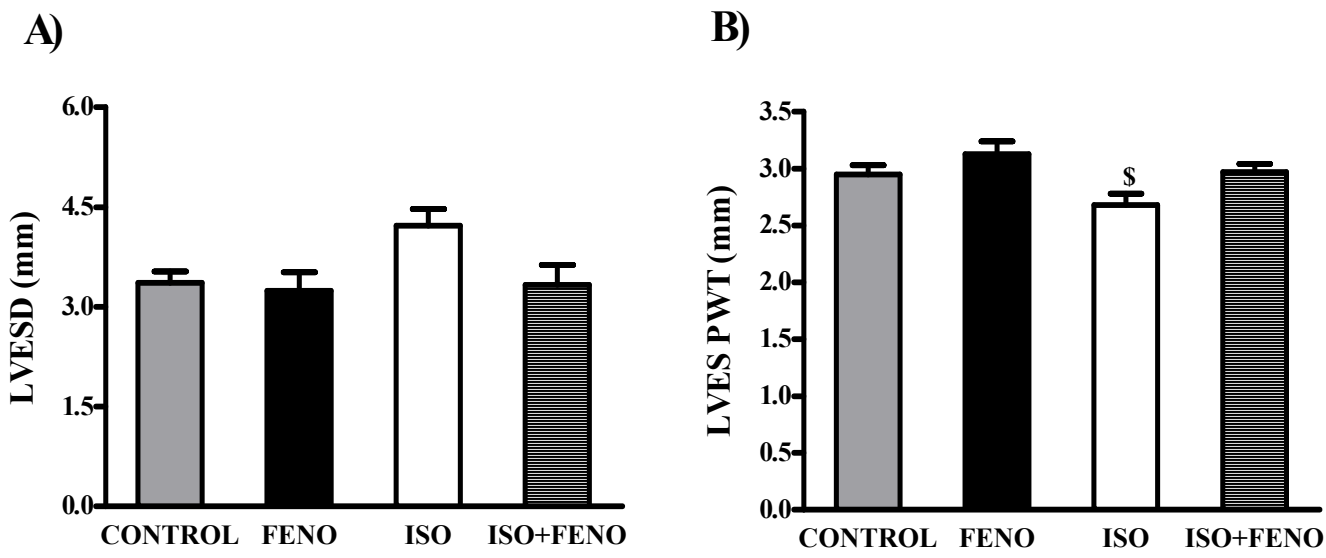

Figure 9. Cardiac systolic dimensions as determined by echocardiography in rats. *Echocardiography was performed following five weeks of isoproterenol and fenofibrate administration in rats to determine cardiac dimensions. A) Left ventricular end systolic diameter (LVESD); B) End systolic posterior wall thickness (LVES PWT). Between-group differences were tested using a one-way ANOVA. n= 6-8. Values are means±SEM.* $^{\$}p<0.05$ *vs. FENO.*

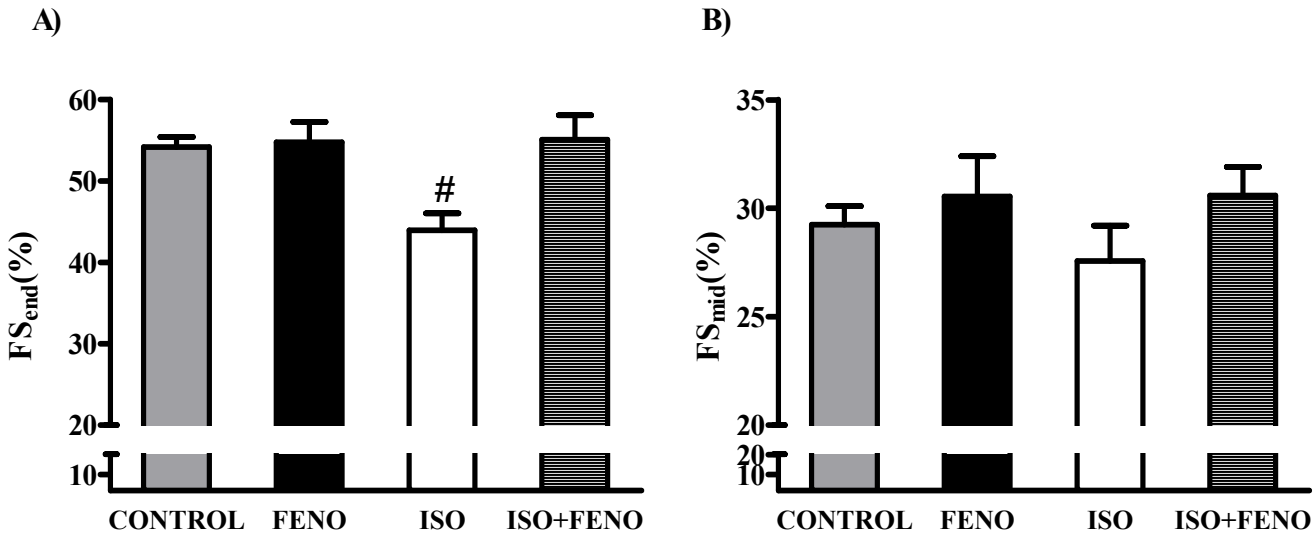

Figure 10. Fenofibrate prevents isoproterenol-induced LV systolic chamber dysfunction. *Echocardiography was performed following five weeks of isoproterenol and fenofibrate treatment in rats to determine cardiac dimensions; these dimensions were then used to determine cardiac function. A) Endocardial fractional shortening (FS_{end}); B) Midwall fractional shortening (FS_{mid}). Between-group differences were tested using a one-way ANOVA. n= 6-8. Values are means±SEM. $^{\#}p<0.05$ vs. CONTROL, FENO AND ISO+FENO.*

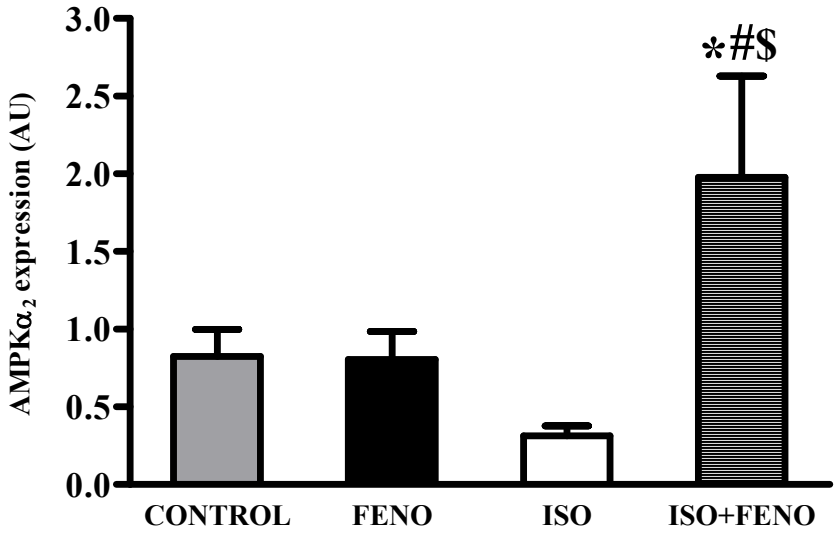

Figure 11. Increased AMPKα$_2$ gene expression following co-administration of isoproterenol and fenofibrate. *Transcript levels were measured in cardiac left ventricular tissue using real-time polymerase chain reaction following five weeks of isoproterenol and fenofibrate administration. Between-group differences were tested using a one-way ANOVA.* ***** *$p<0.05$ vs. control; $^{\#}p<0.01$ vs. ISO; $^{\$}p<0.05$ vs. FENO. n= 8-12. Values are means±SEM, normalized to GAPDH.*

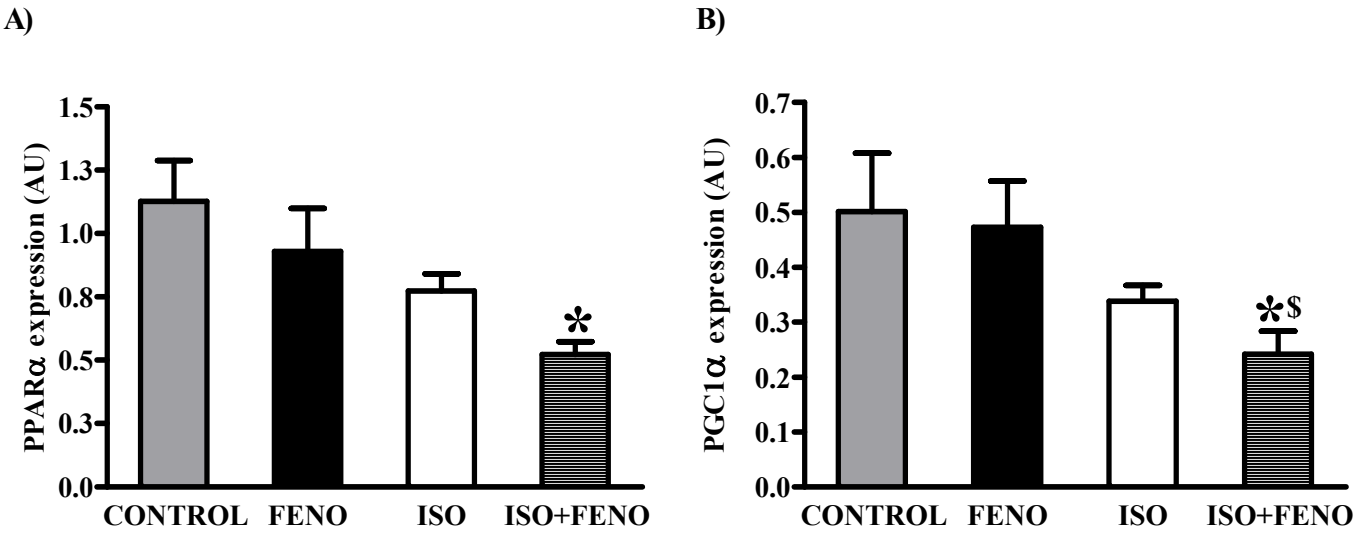

Figure 12. Downregulation of PPARα and PGC-1α gene expression following co-administration of isoproterenol and fenofibrate. *Transcript levels were measured in cardiac left ventricular tissue using real-time polymerase chain reaction following five weeks of isoproterenol and fenofibrate. A) Peroxisome proliferator-activated receptor alpha (PPARα); B) Peroxisome proliferator activated receptor-γ coactivator 1 alpha (PGC-1α). Between-group differences were tested using a one-way ANOVA.* ***p<0.05 vs. CONTROL;* $p<0.05 vs. FENO. *n= 8-12. Values are means±SEM, normalized to GAPDH.*

3.5.3. Co-administration of fenofibrate preserves the mRNA expression of TFAM

TFAM and NRF-1 mRNA expressions were measured since both are key transcription factors in regulation of mitochondrial biogenesis, structure and function; the results are shown in figure 13A and B. There were no significant differences in cardiac NRF-1 expression among all groups (CONTROL, 1.03±0.15; FENO, 1.14±0.13; ISO, 1.11±0.14; ISO+FENO, 1.48±0.20; NS). These results suggest that the mRNA expression of NRF-1 remains unchanged following administration of fenofibrate and isoproterenol.

There was no significant difference in cardiac TFAM mRNA expression between the FENO compared to CONTROL group (CONTROL, 1.75±0.11 vs. FENO, 2.57±0.43; NS). There was also no significant difference in cardiac TFAM mRNA expression between the ISO compared to CONTROL group (CONTROL, 1.75±0.11 vs. ISO, 1.34±0.13; NS). There was no significant difference in TFAM mRNA expression between ISO+FENO and CONTROL group (CONTROL, 1.75±0.11 vs. ISO+FENO, 2.26±0.43; NS), however TFAM mRNA expressions were significantly higher in the fenofibrate-treated groups compared to ISO group (ISO, 1.34±0.13 vs. FENO, 2.57±0.43; $p<0.05$ and ISO, 1.34±0.13 vs. ISO+FENO, 2.26±0.43; $p<0.05$). Taken together, these results suggest that fenofibrate co-administration preserves the mRNA expression of TFAM.

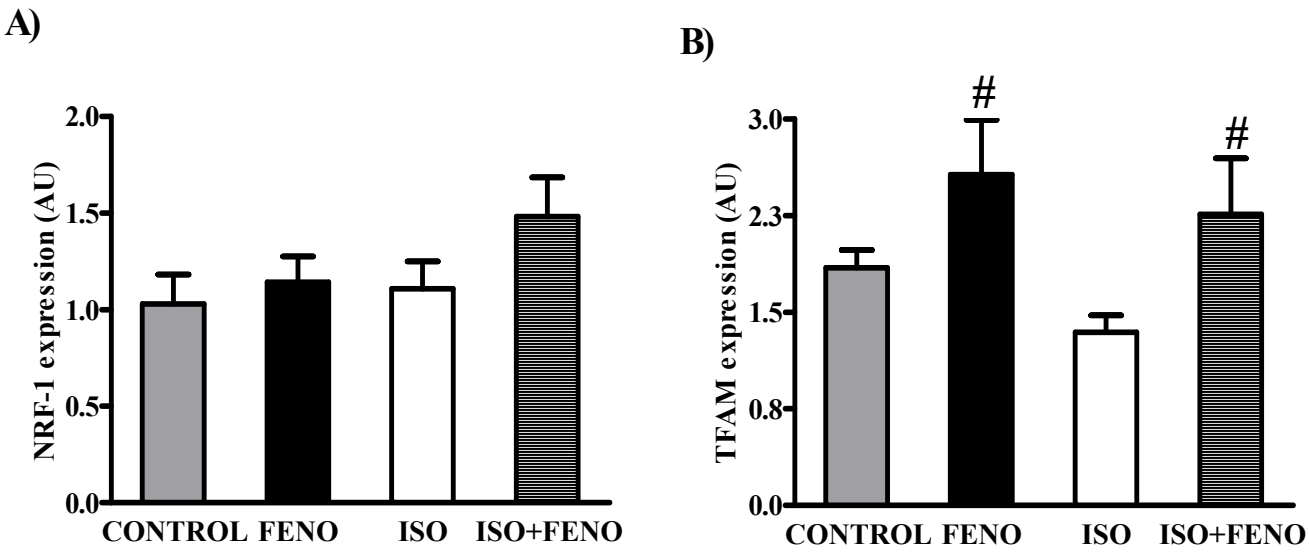

Figure 13. Co-administration of fenofibrate preserves mRNA expression of TFAM. *Transcript levels were measured in cardiac left ventricular tissue using real-time polymerase chain reaction following five weeks of isoproterenol and fenofibrate administration. A) Nuclear respiratory factor-1 (NRF-1); B) Mitochondrial transcription factor A (TFAM). Between-group differences were tested using a one-way ANOVA.* $^{\#}p<0.05$ *vs. ISO. n= 8-12. Values are means±SEM, normalized to GAPDH.*

3.6. Mitochondrial analysis

Electron microscopy was used to determine mitochondrial degeneration and number, which were used as indicators of mitochondrial myopathy and biogenesis.

3.6.1. No evidence of mitochondrial biogenesis following administration of isoproterenol and fenofibrate

Relative mitochondrial area was calculated to determine mitochondrial biogenesis; the results are shown in figure 14. There was no significant difference in relative mitochondrial area between CONTROL compared to ISO group (CONTROL, 0.30±0.01 vs. ISO, 0.26±0.02; NS). There were also no changes in relative mitochondrial area following fenofibrate treatment (CONTROL, 0.30±0.01 vs. FENO, 0.29±0.03; NS and CONTROL, 0.30±0.01 vs. ISO+FENO, 0.34±0.03; NS). Mitochondrial quantitative analysis suggests that isoproterenol and fenofibrate administration had no effect on mitochondrial biogenesis.

3.6.2. Fenofibrate prevents isoproterenol-induced mitochondrial pathology

Micrographs were also examined for the presence of ultrastructural changes. In the CONTROL group, there was normal myofibrillar arrangement with prominent Z-discs, linear arrangement of mitochondria and presence of double layers of mitochondria with normal mitochondrial cristae and no evidence of pathology; figures 15A and 16A. Heart muscle from rats administered with isoproterenol exhibited myofibrillar derangement with absence of Z-discs, mitochondrial derangement, with mostly single layers of mitochondria; areas that had displacement of cristae and vacuolation compared to CONTROL group, figures 15C and 16C. Myofibrillar arrangement, mitochondrial arrangement and cristae density in heart muscle from the ISO+FENO group

resembled that seen in heart muscle from the CONTROL group (Figures 15A and D; figures 16A and D). Therefore, our results suggest that fenofibrate protects against isoproterenol-induced mitochondrial pathology.

3.7. Correlations between gene expression and cardiac function

Correlations were performed to investigate associations between functional changes and metabolic gene regulation; correlations are shown in table 5. There was a positive correlation between AMPKα_2 expression and FS_{end} ($r=0.47$; $p<0.05$), suggesting an association between cardiac pump function and gene expression of AMPKα_2. There were also positive correlations between TFAM expression with FS_{end} ($r=0.51$; $p<0.05$) and FS_{mid} ($r=0.51$; $p<0.05$), suggesting an association between TFAM mRNA expression with cardiac myocardial and pump function. There was a negative correlation between AMPKα_2 and PPARα expressions ($r=-0.32$; $p<0.05$). Similarly, there was a negative correlation between AMPKα_2 and PGC-1α expressions ($r=-0.42$; $p<0.05$). Furthermore, PPARα and PGC-1α expressions were positively correlated ($r=0.46$; $p<0.05$), suggesting that reduced PPARα might have led to corresponding reduction in co-activation by PGC-1α. Correlations between other variables were not significant. Therefore, our results point to associations between cardiac function and key metabolic and mitochondrial gene expressions, AMPKα_2 and TFAM.

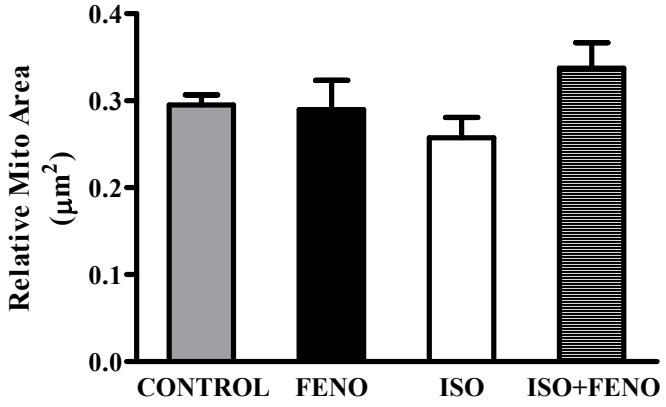

Figure 14. No evidence of mitochondrial (Mito) biogenesis following administration of isoproterenol and fenofibrate. *Quantitative mitochondrial analysis was carried out on electron micrographs. Area (μm^2) covered by mitochondria was calculated relative to total micrograph area to determine mitochondrial biogenesis. Between-group differences were tested using a one-way ANOVA. n= 4 (×4-6 micrographs for each animal). Values are means±SEM.*

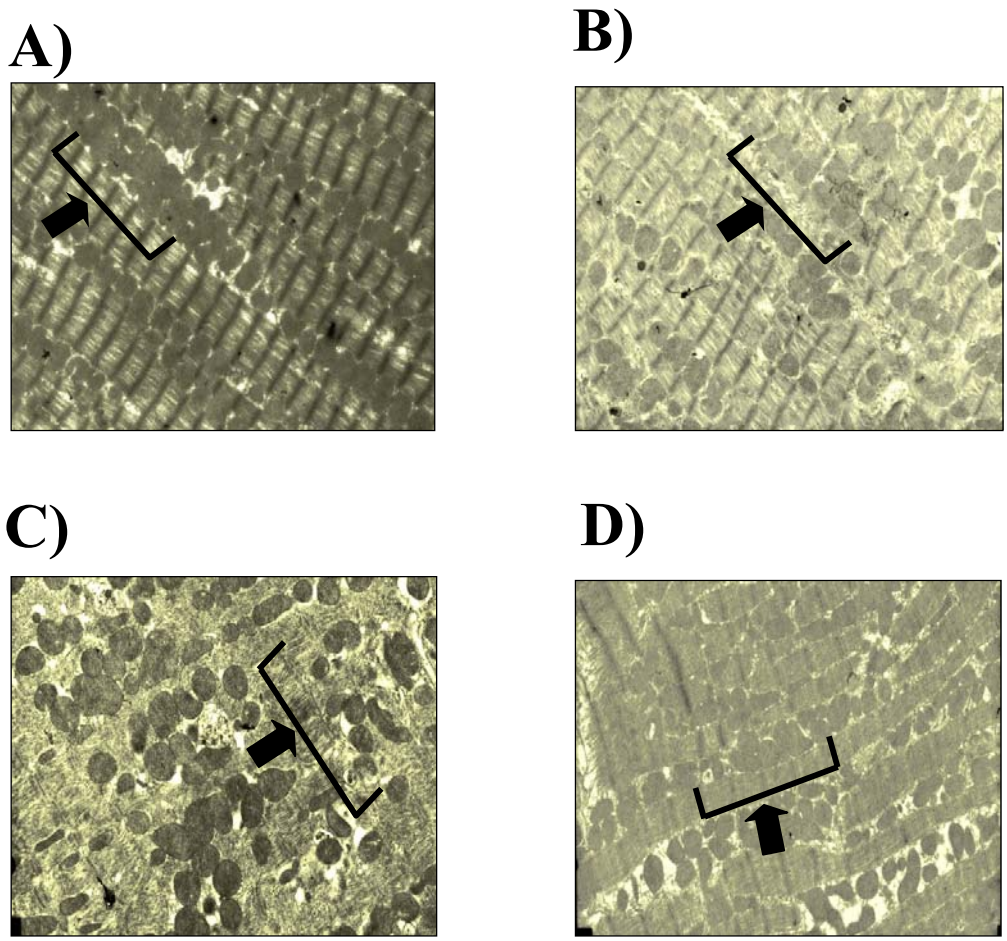

Figure 15. Fenofibrate prevents isoproterenol-induced mitochondrial derangement. *Images were created following transmission electron microscopy of cardiac left ventricular tissue. Magnification: 5000×. A) CONTROL; B) FENO; C) ISO; D) ISO+FENO. Black arrows on A, B and D indicate linear arrangement of mitochondria; the black arrow in C indicates mitochondrial derangement.*

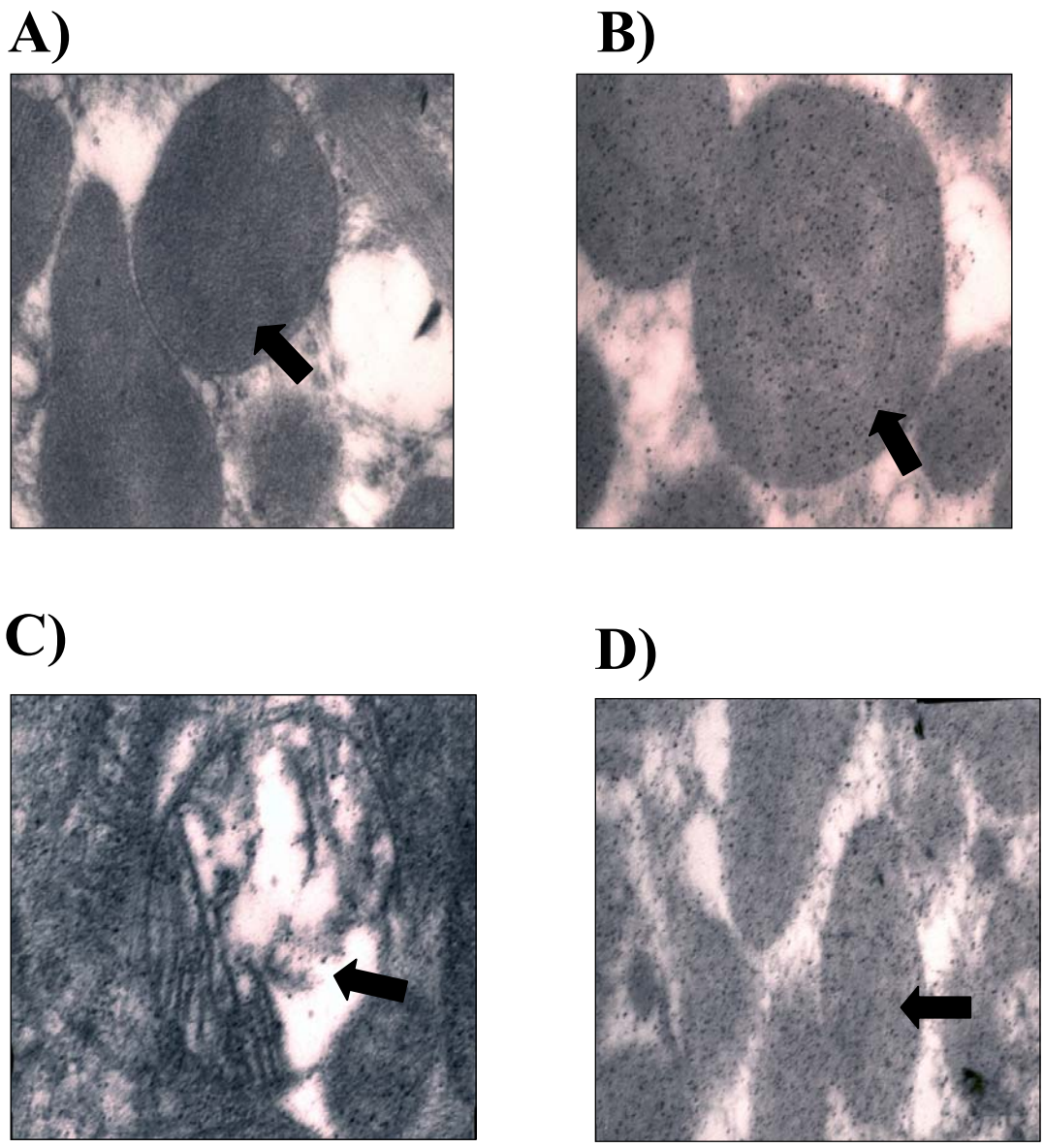

Figure 16. Fenofibrate prevents isoproterenol-induced disruption and swelling of mitochondrial cristae. *Images were created following transmission electron microscopy of cardiac left ventricular tissue. Magnification: 40000×. A) CONTROL; B) FENO; C) ISO; D) ISO+FENO. Black arrows on A, B and D indicate mitochondrial cristae in regular order and tightly packed; the black arrow in C indicates disruption and swelling of mitochondrial cristae.*

Table 5. Correlation coefficients between cardiac function and metabolic gene regulators

	AMPKα$_2$	**PPARα**	**PGC-1α**	**NRF-1**	**TFAM**
LVM/TL	-0.13	-0.07	-0.09	0.28	-0.17
FS_{end}	0.22	-0.01	-0.03	-0.03	0.13
FS_{mid}	0.22	0.06	0.10	0.06	0.10
AMPKα_2	1.00	-0.32*	-0.42*	0.21	0.15
PPARα	-0.32*	1.00	0.46*	0.08	0.29
PGC-1α	-0.42*	0.46*	1.00	0.11	0.30
NRF-1	0.21	0.08	0.11	1.00	0.29
TFAM	0.15	0.29	0.30	0.29	1.00

***p<0.05 for correlation coefficients that were significantly different from zero.*

4. DISCUSSION

4.1. Main outcomes of the study

We have shown that 5-week administration of isoproterenol is associated with left ventricular hypertrophy (LVH) and left ventricular systolic chamber dysfunction (FS_{end}) in rats. Isoproterenol-induced LVH and LV systolic chamber dysfunction was associated with unchanged fasting blood glucose and plasma FFA concentrations. Isoproterenol-induced LVH and LV systolic chamber dysfunction was associated with a decrease of blood TG concentrations. Furthermore, isoproterenol-induced LVH and LV systolic chamber dysfunction were associated with compromised mitochondrial integrity as evidenced by mitochondrial derangements and cristae clearing. However, we did not find any significant changes in mRNA expression of genes involved in mitochondrial fatty acid oxidation (PPARα and AMPKα_2), mitochondrial respiration (NRF-1) and mitochondrial biogenesis (TFAM and PGC-1α) in association with administration of isoproterenol. Importantly, co-administration with fenofibrate prevented isoproterenol-induced deleterious effects such as LVH, LV systolic chamber dysfunction and mitochondrial damage. Notably, fenofibrate-induced cardioprotection was accompanied by an upregulation of AMPKα_2 and TFAM mRNA expressions with a corresponding downregulation of PGC-1α and PPARα mRNA expressions. Collectively, these data suggest that fenofibrate-induced metabolic modulations may confer cardioprotection against detrimental effects of sustained stimulation of the sympathetic nervous system in heart failure.

4.2. Fenofibrate prevents isoproterenol-induced LVH and LV systolic chamber dysfunction

Previous investigators have demonstrated that both chronic and acute administrations of isoproterenol, a β-adrenergic receptor agonist plays a significant role in deleterious processes such as myocardial apoptosis/necrosis, release of pro-inflammatory cytokines and oxidative stress (Davel et al 2008, Jin et al 2007, Murray et al 2000, Mohan et.al. 1999 and Shizukuda et al 1998). Interestingly, activation of these processes has been associated with cardiac remodelling and dysfunction. Also, sustained stimulation of the SNS is a well-established characteristic of progressive heart failure (Eisenhofer et al 1996 and Dzau et al 1983). In agreement with others, here we have demonstrated that sustained SNS stimulation alone could induce the development of left ventricular dysfunction. Since stimulation of SNS is associated with increased breakdown of TGs and increased plasma FFA concentrations, some have previously suggested that a subsequent increase in intracellular FFAs may contribute to cardiac dysfunction (Listenberger et al 2002 and Lopaschuk et al 1994). In our study, we showed no changes in plasma FFAs following chronic administration of isoproterenol but, according to Mohan and Bloom (1999), isoproterenol-induced elevation of FFAs lasts for about four hours, and thereafter returns to normal levels. Since we measured FFAs 24 hours after the last isoproterenol injection, it is likely that we missed an earlier surge in plasma FFAs. It may also be that a significant decrease in circulating TG concentrations in these rats bears testimony to the existence of isoproterenol-induced lipolysis despite missing the surge of FFAs at the time of blood collection. Interestingly, Mohan and Bloom (1999) have also demonstrated that a short-term increase in isoproterenol-induced FFA concentrations leads to myocardial necrosis. Here, inhibitors of lipid mobilization, fatty acid utilization and lipid peroxidation blunted isoproterenol-mediated myocardial necrosis; however, simultaneous infusion of lipases with isoproterenol worsened myocardial necrosis

(Mohan and Bloom, 1999). In other studies, isoproterenol-mediated myocardial necrosis was associated with cardiac remodelling as evidenced by the presence of left ventricular hypertrophy in rat hearts (Zhang et al 2008a and Goldspink et al 2004). In agreement with these studies, we also demonstrated that low dose administration of isoproterenol resulted in LVH. It is thus conceivable that chronic but intermittent β-adrenergic receptor stimulation with isoproterenol predisposes the heart to myocardial necrosis and LVH, in part, via the transient but detrimental effects of FFA surge.

In that regard, increased availability and cellular uptake of FFAs might lead to increased mitochondrial FA oxidation and subsequent stimulation of proapoptotic signals such as cytochrome c release and caspase-3 activation, thereby accelerating the onset of cardiomyocyte apoptosis (Kong and Rabkin, 2004). Indeed, apoptosis is said to be a major contributor to cardiac dysfunction in heart failure (Shizukuda et al 1998). Importantly, both chronic and acute administrations of isoproterenol have been demonstrated as potential triggers of apoptosis (Ding et al 2005 and Shizukuda et al 1998). Whether this potential deleterious effect is also linked to the previously reported surge of FFAs is not fully understood. However, previous studies suggest that isoproterenol and catecholamines may induce apoptosis via mechanisms such as lipid peroxidation and oxidative stress.

Although we did not observe any significant differences in the expression of genes regulating mitochondrial energy metabolism following isoproterenol administration in this study, others have demonstrated an association between isoproterenol-induced LVH and metabolic dysfunction (Heather et al 2009). However, there's uncertainty as to whether metabolic dysfunction observed by Heather (2009) is linked to isoproterenol-mediated oxidative stress. Interestingly, increases in the oxidant stimulant-to-oxidant inhibitor ratio contributed to heart

failure in several experimental models (Qin et al 2003 and Nakamura et al 2002). To demonstrate this, administration of vitamin C, a well-recognized anti-oxidant, attenuated isoproterenol-induced myocardial damage (Mohan and Bloom, 1999). It is therefore possible that in the current study, isoproterenol will have contributed to LV remodelling and LV systolic chamber dysfunction, in part, via stimulation of these oxidative stress and pro-apoptotic mediators.

Having said that, in this study, fenofibrate prevented the onset of LVH and preserved LV systolic function. This is in agreement with other studies where fenofibrate prevented cardiac remodelling and systolic chamber dysfunction (Duhaney et al 2007, LeBrasseur et al 2007 and Diep et al 2004). Whether these beneficial effects of fenofibrate are indirectly related to PPARα activation is still a matter of intense debate; however, fenofibrate has been shown to be cardioprotective in various models of heart failure (Smeets et al 2008a and Diep et al 2004). Infusion of fenofibrate attenuated angiotensin-II induced production of pro-inflammatory mediators and partially prevented fibrosis via inhibition of transforming growth factor-β1 and collagen deposition (Diep et al. 2004). It is also worth noting that fenofibrate-mediated regulation of protein synthesis has been demonstrated to prevent endothelin-1 (ET-1) induced cardiomyocyte hypertrophy (Liang et al 2003).

Fenofibrate could also prevent the induction of cardiac damage via inhibition of cardiomyocyte apoptosis and lipid peroxidation (De Silva et al 2009 and Ichihara et al 2007). Although it is unclear whether fenofibrate prevents apoptosis independent of PPARα activation, another PPARα agonist, WY14643, which produces a greater expression of PPARα, was also shown to suppress cardiomyocyte apoptosis (Wu et al 2010 and Yeh et al 2006). Despite these beneficial effects, PPARα activation has also been shown to produce apoptosis, however, these toxic effects seem to be cell-type specific and/or disease specific (Zhao et al 2010). For instance,

PPARα-/- mice are more susceptible to hypertrophic stimulation by chronic pressure overload and exhibit inflammation, extracellular matrix remodelling and cardiac dysfunction (Smeets et al 2008b and Duhaney et al 2007). Importantly though, it is worth noting that whole body deletion of PPARα would severely limit the role of the liver in clearance of circulating FFAs and cardiac metabolic switching. Therefore, whole body deletion of PPARα would make the heart even more susceptible to adverse metabolic remodeling. This indicates the importance of the presence of PPARα in conferring cardioprotection. Having said that, overexpression of PPARα in mice hindered cardiac recovery in reperfusion following ischaemia and this was associated with excessive fatty acid oxidation (Sambandam et al 2006). In support, cardiomyopathy in PPARα overexpressing mice has been likened to that seen in diabetes since both disease models are associated with excess FFAs uptake and hence excessive fatty acid oxidation (Hopkins et al 2003, Chiu et al 2001 and Finck et al 2002). Although, in the current study, PPARα gene expression was significantly reduced following co-administration of isoproterenol and fenofibrate, it is unclear how fenofibrate conferred cardioprotection. Perhaps fenofibrate confers cardioprotection against LVH and LV dysfunction via inhibition of isoproterenol-induced pro-inflammatory and pro-apoptotic processes.

4.3. Fenofibrate preserves mitochondrial integrity against isoproterenol-induced damage

Several studies have attributed poor contractile function observed in progressive heart failure to loss of mitochondrial integrity (Dabkowski et al 2009 and Schaper et al 1991). In this study, we investigated mitochondrial morphology and density together with gene expression of TFAM, a transcription factor that plays a prominent role in maintenance of mitochondrial integrity and

function (Xu et al 2009 and Suarez et al 2008). Although there were no significant changes in relative mitochondrial density amongst all the groups, characteristics of mitochondrial damage as evidenced by mitochondrial derangements and cristae clearing were associated with isoproterenol-induced LVH and LV dysfunction. Clearing of cristae has previously been reported in isoproterenol-induced myocardial infarction (Rajadurai and Prince, 2007). Previous investigators had demonstrated that mitochondrial number, size and structural arrangement are altered in human end-stage dilated cardiomyopathy and that perhaps these changes occur belatedly in the development of heart failure (Murray et al 2008, Bugger et al 2006 and Schaper et al 1991). Others have suggested that mitochondrial dysfunction may precede cardiac dysfunction (Zoll et al 2006 and Javadov et al 2005). In agreement, we found that isoproterenol-induced LVH and LV systolic chamber dysfunction was accompanied by mitochondrial pathology.

In light of the fact that isoproterenol provokes cardiac oxidative stress via ROS generation (Zhang et al 2005), we can therefore speculate that ROS-mediated mitochondrial damage may have led to reduced cardiac efficiency in this study. Others have also implicated increased generation of ROS in the progression of cardiac hypertrophy and heart failure (Dhalla et al 2000, Chien et al 1999 and Sugden et al 1998). Kang et al (2007) went even further to suggest that mtDNA is the primary target of ROS generated by the respiratory chain due to its close proximity to the ETC. Importantly, under conditions that promote cardiac oxidative stress, TFAM has been noted to play a critical compensatory role in stabilizing mtDNA (Larsson et al 1998). Given this, it is therefore not far-fetched to assume that isoproterenol may target mtDNA, as evidenced by mitochondrial damage in this study. Perhaps the unchanged expression of TFAM observed in this study could have been because of an effort to maintain mtDNA stability.

However, future studies are required to evaluate this potential mechanism. Having said that, others have also shown a clear association between decreased TFAM expression and mitochondrial dysfunction in other rat models of progressive heart failure (Javadov et al 2006, Garnier et al 2003 and Barger et al 2000). In these studies, cardiac deletion of TFAM in mice is characterized by a significant decrease in mtDNA content and dilated cardiomyopathy (Wang et al 1999). However, TFAM-mediated attenuation of chamber dilatation and cardiac dysfunction is accompanied by attenuation of myocyte hypertrophy, fibrosis and apoptosis (Ikeuchi et al 2005). In support of this argument, isoproterenol-induced or catecholamine-mediated mitochondrial derangement and clearing of cristae have also been shown in other studies to be a possible mechanism of isoproterenol-induced cardiac dysfunction (Yogeeta et al 2008 and Sabbah et al 1992). Although we did not measure mtDNA and that TFAM gene expression was unchanged, we have nevertheless demonstrated that isoproterenol-induced LVH and LV systolic chamber dysfunction was accompanied by mitochondrial damage. Perhaps our studies point to an early onset of cardiac dysfunction because LVH, as an adaptive response to an insult, is usually not accompanied by chamber dysfunction unless cardiac decompensation has started to emerge. Importantly, our method of mitochondrial quantification did not allow for separation of efficient and dysfunctional mitochondria. Moreover, gene expression of transcription factors involved in the regulation of mitochondrial respiration and mitochondrial biogenesis, NRF-1 and PGC-1α respectively, were unchanged following isoproterenol-induced LVH and LV dysfunction.

4.4. Fenofibrate may protect against isoproterenol cardiac damage via metabolic remodelling

In several experimental models of cardiac hypertrophy and heart failure, downregulation of genes responsible for FA uptake and utilization has been reported (Akki et al 2008, Osorio et al 2002, Razenghi et al 2001, Taylor et al 2001 and Rossenblatt-Vlein et al 2001). However, isoproterenol-induced LVH and LV dysfunction was not associated with any significant changes in mRNA expression of genes involved in mitochondrial fatty acid oxidation (PPARα and AMPKα_2), mitochondrial respiration (NRF-1) and mitochondrial biogenesis (PGC-1α and TFAM). It has been shown elsewhere that isoproterenol-induced metabolic effects may last for a very short period of time i.e. elevation of FFAs lasts for four hours (Mohan and Bloom, 1999). As previously explained, sample collection in our study occurred 24 hours after the last dose of isoproterenol; given that isoproterenol-induced effects on FFAs lasts for a short period of time, it is therefore possible that we also missed isoproterenol-induced metabolic gene changes.

It is also worth pointing out that the differences in metabolic remodelling seem to depend on type and duration of the hypertrophic stimulus and/or type and severity of the disease model. For instance, Akki et al (2008) showed that cardiac hypertrophy induced by abdominal aortic constriction is accompanied by a down-regulation of FAO oxidation genes such as PPARα, mCPT-1, MCAD, UCP3 and PDK4. Furthermore, Akki and colleagues suggested that metabolic gene changes represent an earlier stage of hypertrophy since these changes were not accompanied by myocardial functional deterioration in their study. In support, previous investigators have suggested that metabolic gene downregulation occurs as early as 48 hours following a hypertrophic stimulus and therefore these initial metabolic changes are thought be part of an adaptive response against functional deterioration (van den Bosch et al 2006).

Conversely, van den Bosch (2006) did not demonstrate any changes in metabolic gene regulation after two, three and eight weeks of transverse aortic constriction (TAC)-induced cardiac hypertrophy (van den Bosch et al 2006). Despite these inconsistencies, several studies of rat models of metabolic disorders have consistently yielded results that suggest a strong association between metabolic perturbations and undesirable cardiovascular outcomes (Yan et al 2009 and Buchanan et al 2005). Several investigators have suggested that modulation of cardiac metabolism with pharmacological agents such as fenofibrate and metformin may have a protective effect against metabolic perturbations observed in some models of heart failure (Baraka and AbdelGawad, 2010; Sasaki et al 2009, Forcheron et al 2009 and Ichihara et al 2006).

Interestingly, we have shown that fenofibrate prevents isoproterenol-induced LVH and LV systolic chamber dysfunction. Our results suggest that fenofibrate protects against isoproterenol-induced deleterious effects, in part, via differential regulation of key metabolic genes and preservation of cardiac mitochondrial integrity. Here, we also demonstrated that fenofibrate-mediated cardioprotection was accompanied by downregulation of cardiac PPARα mRNA expression. Our observations, in this regard, are in contrast with previous findings where fenofibrate was identified as a PPARα agonist (LeBrasseur, 2007 and Duhaney, 2007). Having said that, inconsistencies between hepatic and cardiac expressions of PPARα controlled genes following in-vivo fenofibrate administration have been noted in previous studies (Aasum et al 2008 and Verreth et al 2006). Although it may sound counterintuitive to observe differential regulatory effects of fenofibrate on PPARα, these disparities seem to depend on whether fenofibrate was administered *in vitro* (Van der Lee et al 2000 and Brandt et al 1998) or *in vivo* (Aasum et al 2008 and Kim et al 2003) or the duration of drug administration (Labinskyy et al

2007, Morgan et al 2005, Xu et al 2006 and Diep et al 2004). These studies suggest that *in vitro* or acute administration tends to result in a direct effect on PPARα activation while *in vivo* or chronic administration leads to differential PPARα regulation in the heart and liver. For example, *in vivo* administration of fenofibrate significantly increased PPARα expression in the liver or adipose tissue while cardiac PPARα remained unchanged (Aasum et al 2008, Verreth et al 2006 and Morgan et al 2005). Furthermore, liver fatty acid oxidation was also increased while cardiac fatty acid oxidation was significantly decreased following systemic fenofibrate treatment in diet-induced obese (DIO) mice (Aasum et al 2008). Here, Aasum et al (2008) suggest that PPARα expression in the heart could be a secondary occurrence since PPARα activity primarily occurs in the liver, a primary metabolic organ that utilizes circulating lipids for either fatty acid oxidation or synthesis. Thus, whole body administration of fenofibrate would primarily and preferentially activate PPARα in the liver thereby causing hepatic lipid drainage. Since liver PPARα is a key transcription factor that regulates metabolic genes involved in key fatty acid utilization pathways, a decrease in fatty acid oxidation in other metabolically active organs such heart and skeletal muscle could therefore be explained by either reduced availability of circulating FFAs or fenofibrate-induced switch in cardiac metabolism from fatty acid oxidation to glucose oxidation. Given that FFAs serve as natural ligands for PPARα, increased clearance of circulating FFAs by the liver may result in downregulation of PPARα expression and its target FAO genes in other metabolically active tissues such as the heart. However, there were no significant changes in FFA concentrations following fenofibrate administration in this study. Although FFAs were unchanged, gene expressions of both cardiac PPARα and PGC-1α, master transcriptional regulators of fatty acid uptake and utilization, were significantly decreased implying that a decrease in myocardial fatty acid oxidation may have occurred following co-

administration with fenofibrate. Importantly, the positive association between PPARα and PGC-1α gene expressions in our study supports earlier findings that co-activation of PPARα and PGC-1α transcriptionally regulates metabolic genes involved in fatty acid uptake and utilization. In the current study, reduced cardiac uptake of FFAs via PPARα-regulated cell membrane bound fatty acid transporters such as FAT, FABP and FAT/CD36 could lead to reduced intracellular FFAs (natural PPARα ligands) and subsequent reduction in cardiac PPARα and PGC-1α gene expressions. If this is the case, unchanged circulating FFAs as opposed to reduced circulating FFAs could be attributed, in part, to reduced cellular FFA uptake, however this idea remains to be tested. Having said that, metabolic remodelling away from FAO but towards glucose oxidation following fenofibrate co-administration cannot be ruled out. In support, fenofibrate co-administration resulted in significant reductions in cardiac PPARα and PGC-1α gene expressions. Similar observations were noted by other investigators (Yuan et al 2008 and Aasum et al 2002). In this regard, and in agreement with our speculations, others have demonstrated that alterations in myocardial substrate metabolism, (i.e. improved glucose uptake and utilization accompanied by reduced FAO) following fenofibrate treatment are associated with improved cardiac function by possibly preventing myocardial FFA accumulation (Kim et al 2003; LeBrasseur et al 2007). It is also worth noting that fenofibrate could have prevented chamber dysfunction via a reduction in mitochondrial FAO metabolic demand, here both transcriptional regulators of FA metabolism, PPARα and PGC-1α, were significantly lowered. Previous investigators have also indicated that increased and long-term reliance on mitochondrial FAO imposes metabolic stress, which predisposes the heart to cardiac dysfunction (Finck et al 2002, Chiu et al 2001 and Zhou et al 2000).

4.5. The role of AMPKα_2 in fenofibrate-induced cardioprotection

AMPK, a key metabolic regulator of cellular energy homeostasis is activated under metabolic stress and has been shown to play a central role in regulating cardiac metabolism in various models of cardiac hypertrophy. In this study, we did not find any changes in AMPKα_2 mRNA expression in the isoproterenol-induced LVH and LV systolic chamber dysfunction. AMPKα_2 is said to be activated in conditions of low ATP synthesis such as ischaemia and oxidative stress (Young et al 2005 and Kahn et al 2005). We suspect that at this stage of isoproterenol-induced LVH and LV systolic chamber dysfunction, metabolic remodelling and decrease in ATP was mild and did not reach a high enough AMP:ATP ratio to stimulate an increase in activity of AMPKα_2. In the transverse aortic constriction (TAC) model, deletion of AMPKα_2 was associated with worsened LVH and LV systolic chamber dysfunction in mice (Zhang et al 2008b). Zhang et al (2008b) suggested that AMPKα_2 might have a cardioprotective role against myocardial fibrosis and increased cardiomyocyte size following TAC. Further, LVH induced by administration of high dose (50 $mg.kg^{-1}.day^{-1}$) isoproterenol for seven days was found to be greater in AMPKα_2-null mice compared to wild-type mice (Zarrinpashnesh et al 2008). Here, the absence of AMPKα_2 was associated with increased activation of enzymes involved in stimulation of cardiomyocyte growth namely; for example, P70 ribosomal S6 protein kinase (Zarrinpashnesh et al 2008). Zarrinpashnesh et al (2008) have also shown that high dose isoproterenol induced LVH that was associated with unchanged AMPKα_2 mRNA expression, a finding similar to ours.

Furthermore, relative upregulation of AMPKα_2 mRNA expression following co-administration with fenofibrate points to a metabolic switch away from fatty acid metabolism in favour of glucose metabolism. Such an assertion is further supported by the negative association between AMPKα_2 and PPARα / PGC-1α mRNA expressions. Although we did not measure expression of

genes that regulate glucose metabolism in this study, a decrease of fatty acid metabolism is known to result in a compensatory increase of glucose metabolism. AMPKα_2 has indeed been shown to facilitate glucose metabolism via translocation of muscle glucose transporter 4 (GLUT4) and activation of phosphofructokinase (PFK) 2 (Yamaguchi et al 2005). AMPKα_2 can also increase FA oxidation through regulation of ACCβ (Kudo et al 1995). In our study, a concurrent decrease in FA-responsive genes such as PPARα and PGC-1α in the heart supports our assertion that fenofibrate induced a shift towards glucose metabolism and that this shift led to activation of AMPKα_2 and hence cardioprotection. Although earlier findings point to positive associations between AMPKα_2 and PPARα / PGC-1α (Lee et al 2006; Baar, 2004 and Zong et al 2002), it is important to indicate that these associations were established in skeletal muscle and the heart may respond differently to structural and functional changes.

Stimulation of AMPKα_2 has also been shown to be protective against functional deterioration caused by ischaemia through metabolic adaptations (Russell et al 2004b). Additionally, AMPKα_2 activation has previously been shown to be part of a protective mechanism against cardiac hypertrophy in different experimental studies. Shibata et al (2004) and Sidhu et al (2005) suggested that AMPKα_2 inhibits cardiomyocyte growth, thereby preventing myocardial hypertrophy. Gauthier et al (2008) showed that without an increase in AMPKα_2, isoproterenol-induced lipolysis was associated with energy depletion and an increase in ROS generation. In support of the positive role of AMPKα_2, we found strong positive associations between AMPKα_2 mRNA expression and myocardial and systolic function measurements. Therefore, our results suggest that the protective actions of fenofibrate against isoproterenol-induced LVH and LV systolic chamber dysfunction possibly require upregulation of AMPKα_2 mRNA expression. However, we are still uncertain as to whether fenofibrate directly activates AMPKα_2 mRNA

expression via a PPARα-independent mechanism or through metabolic switching as our results indicate.

Despite its prominent role in FA metabolism, little is known about the role of AMPKα_2 following administration of a PPARα agonist in vivo. Previously, fenofibrate was shown to increase AMPKα_2 independently of PPARα in human umbilical vein endothelial cells (Murakami et al 2006). Another PPARα agonist, WY-14,643 stimulated AMPKα_2 mRNA expression in hepatoma cells (Liangpunsakul et al 2009); however, it is still to be determined through what mechanisms this stimulation occurs. Nonetheless, an increase in AMPKα_2 mRNA expression was associated with an unchanged ratio of AMP:ATP, suggesting that a WY-14,643-induced increase in AMPKα_2 may be independent of PPARα activity (Liangpunsakul et al 2009). In our study, cardiac increase in AMPKα_2 mRNA expression following *in vivo* administration of fenofibrate was associated with decreased PPARα mRNA expression, thereby supporting the idea of a possible PPARα independent mechanism of cardioprotection.

However, *in vivo* β-adrenergic stimulation leads to increased AMP:ATP ratio and AMPK activity in rat adipocytes (Koh et al 2007). *In vitro*, β-adrenergic stimulation of adipocytes using isoproterenol causes an increase of AMP:ATP ratio by inducing ATP lowering (Gauthier et al 2008). As established, isoproterenol induces lipolysis; a significant proportion of FFAs released via lipolysis undergo reesterification to synthesise TGs, and it is this reesterification that consumes a lot of ATP in adipocytes, thereby increasing AMP:ATP ratio (Brooks et al 1982 and Vaughan, 1962). Therefore, it is very likely that in our study, an exaggerated increase in AMPKα_2 mRNA expression could have been because of a synergistic effect of fenofibrate and isoproterenol on the myocardium.

5. CONCLUSION

5.1. Summary and conclusions

In summary, the chronic administration of isoproterenol induced LVH, which was accompanied by LV systolic chamber dysfunction. LVH and LV systolic chamber dysfunction were associated mitochondrial pathology. Our study also provides evidence that fenofibrate co-administration prevented isoproterenol-induced LVH and LV systolic chamber dysfunction possibly via preserving TFAM expression and mitochondrial architecture. Interestingly, fenofibrate co-administration also seems to bring about metabolic switching away from FAO but towards glucose metabolism perhaps via upregulation of AMPKα_2 mRNA expressions. Interestingly, fenofibrate may protect against isoproterenol-induced LVH and LV systolic chamber dysfunction by preventing inflammation, oxidative stress and fibrosis.

These data are in agreement with the commonly held view that metabolic energy remodelling plays an important role in cardiac hypertrophy and dysfunction. Our findings suggest that in addition to hypolipidaemic effects, PPARα agonists may protect against cardiac remodelling via preservation of mitochondrial structure and function.

5.2. Limitations and future studies

Although findings from this work may assist in filling important gaps in our knowledge of the interaction between cardiac function and metabolic regulatory parameters, the study may have some important limitations. For example, our results and others' suggest that the actions of a

PPARα agonist following *in vivo* administration in the heart may be primarily carried out in the liver, a primary metabolic organ. Therefore, understanding of the liver metabolic gene profile would have been interesting. Further, some studies have shown that it is possible to have disparities between gene and protein expression. Thus, it would be worthwhile, perhaps in future studies to confirm the actions of metabolic genes by also measuring protein expression. It is also worth mentioning that we did not directly measure mitochondrial function to complement mitochondrial gene changes and mitochondrial architecture. It must be remembered that some of the measurements involve *ex vivo* perfusion and would have rendered the tissue inadequate for gene expression studies. Our study could not rule out the possibility that the actions of fenofibrate could have been because of inhibition of processes such as apoptosis, inflammation and oxidative stress, all of which can be induced by isoproterenol. While our study focused mainly on the chronic effects of isoproterenol administration, isoproterenol transiently increases plasma FFA concentrations (Mohan and Bloom, 1999) and it is possible that other effects of isoproterenol, possibly mediated by this FFA surge are also transient. Thus, sample collection conducted less than four hours rather than 24 hours after isoproterenol administration could have yielded different results. Also, a small sample size possibly led to low statistical power and therefore inability to detect significant differences between the groups; that may well have been the case with the mRNA expression data. We acknowledge that an important limitation could be the fact that there was no saline-injected control group and/or a control given plain gelatine cubes only. The effects of plain gelatine cubes on the study of this nature are unknown, while injections may cause inflammation and a possible interference with the results. We further acknowledge that during the terminations, it is possible that some of the animals could have died

from blood loss following incision, rather than the anaesthetic overdose; however, we are unaware as to how that could interfere with results in our study.

With these limitations in mind, we are planning to validate the mitochondrial gene expression and architecture data by measuring mtDNA, kits for these experiments have already been purchased. It could also be interesting to determine to what extent inflammation contributed to isoproterenol-induced LVH. The role of inflammation could be determined by measuring the concentration of pro-inflammatory cytokines or C-reactive protein. We also intend studying gene expression following a longer period of isoproterenol and fenofibrate administration. For instance, four months of isoproterenol administration mimics chronic heart failure with greater functional deficits (unpublished data). It would be interesting to determine the expression of other fatty acid metabolic genes such as CPT-1, ACCβ and MCAD in the isoproterenol model at this stage of cardiac remodelling.

6. REFERENCES

Aasum E, Belke D, Severson D, Riemersma R, Cooper M, Andreassen M & Larsen T. (2002). Cardiac function and metabolism in Type 2 diabetic mice after treatment with BM 17.0744, a novel PPAR-alpha activator. Am J Physiol Heart Circ Physiol 283, 949-957.

Aasum E, Khalid A, Gudbrandsen O, How O, Berge R & Larsen T. (2008). Fenofibrate modulates cardiac and hepatic metabolism and increases ischemic tolerance in diet-induced obese mice. J Mol Cell Cardiol 44, 201-209.

Akki A, Smith K & Seymour A-M. (2008). Compensated cardiac hypertrophy is characterised by a decline in palmitate oxidation. Mol Cell Biochem 311, 215–224.

Baar K. (2004). Involvement of PPAR gamma co-activator-1, nuclear respiratory factors 1 and 2, and PPAR alpha in the adaptive response to endurance exercise. Proc Nutr Soc 63, 269–273.

Badenhorst D, Veliotes D, Maseko M, Tsotetsi O, Brooksbank R, Naidoo A, Woodiwiss A & Norton G. (2003). Adrenergic activation initiates chamber dilatation in concentric hypertrophy. Hypertension 41, 499–504.

Baraka A & AbdelGawad H. (2010). Targeting apoptosis in the heart of streptozotocin-induced diabetic rats. J Cardiovasc Pharmacol Ther 15, 175-181.

Barger P & Kelly D. (2000). PPAR signaling in the control of cardiac energy metabolism. Trends Cardiovasc Med 10, 238–245.

Barger P, Brandt J, Leone T, Weinheimer C & Kelly D. (2000). Deactivation of peroxisome proliferator-activated receptor-alpha during cardiac hypertrophic growth. J Clin Invest 105, 1723-1730.

Beltrami C, Finato N & Rocco M. (1995). The cellular basis of dilated cardiomyopathy in humans. J Mol Cell Cardiol 27 291–305.

Beltrami C, Finato N, Rocco M, Feruglio G, Puricelli C, Cigola E, Quaini F, Sonnenblick E, Olivetti G & Anversa P. (1994). Structural basis of end-stage failure in ischemic cardiomyopathy in humans. Circulation 89, 151-163.

Berg B & Harmison C. (1958). Growth, disease, and aging in the rat. J Gerontol 13, 370-377.

Berger J & Moller D. (2002). The mechanisms of action of PPARs. Annu Rev Med 53, 409–435.

Bergeron R, Ren J, Cadman K, Moore I, Perret P, Pypaert M, Young L, Semenkovich C & Shulman G. (2001). Chronic activation of AMP kinase results in NRF-1 activation and mitochondrial biogenesis. Am J Physiol Endocrinol Metab 281, 1340–1346.

Bing R, Siegel A, Ungar I & Gilbert M. (1954). Metabolism of the human heart. II. Studies on fat, ketone and amino acid metabolism. Am J Med 16, 504-515.

Boudina S, Sena S, Theobald H Sheng X, Wright JJ, Hu XX, Aziz S, Johnson JI, Bugger H, Zaha VG & Abel ED. (2007). Mitochondrial energetics in the heart in obesity related diabetes: direct evidence for increased uncoupled respiration and activation of uncoupling proteins. Diabetes Care 56, 2457–2466.

Braissant O, Foufelle F, Scotto C, Dauça M & Wahli W. (1996). Differential expression of peroxisome proliferator-activated receptors (PPARs): tissue distribution of PPAR-alpha, -beta, and -gamma in the adult rat. Endocrinology 137, 354–366.

Brandt J, Djouadi F & Kelly D. (1998). Fatty acids activate transcription of the muscle carnitine palmitoyltransferase I gene in cardiac myocytes via the peroxisome proliferator-activated receptor alpha. J Biol Chem 273, 786–792.

Braunwald E. (2001). The Denolin Lecture: Congestive heart failure: a half century perspective. Eur Heart J 22, 825-836.

Brigadeau F, Gele P, Wibaux M, Marquie C, Martin-Nizard F & Torpier G. (2007). The PPAR[alpha] activator Fenofibrate slows down the progression of the left ventricular dysfunction in porcine tachycardia-Induced cardiomyopathy. J Cardiovasc Pharmacol 49, 408–415.

Bristow M, Gilbert E, Abraham W, Adams K, Fowler M, Hershberger R, Kubo S, Narahara K, Ingersoll H, Krueger S, Young S & Shusterman N. (1996). Carvedilol produces dose-related improvements in left ventricular function and survival in subjects with chronic heart failure. MOCHA Invest Circ 94, 2807–2816.

Brooks B, Arch J & Newsholme E. (1982). Effects of hormones on the rate of the triacylglycerol/fatty acid substrate cycle in adipocytes and epididymal fat pads. FEBS Lett 146, 327–330.

Brownlee M. (2001). Biochemistry and molecular cell biology of diabetic complications. Nature 414, 813-820.

Bruce C, Brolin C, Turner N, Cleasby M, van der Leij F, Cooney G & Kraegen E. (2006). Overexpression of carnitine palmitoyltransferase 1 (CPT1) in skeletal muscle in vivo increases fatty acid oxidation and reduces triacylglycerol esterification. Am J Physiol Endocrinol Metab 292, 1231-1237.

Buchanan J, Mazumder P, Hu P, Chakrabarti G, Roberts M, Yun U, Cooksey R, Litwin S & Abel E. (2005). Reduced cardiac efficiency and altered substrate metabolism precedes the onset of hyperglycemia and contractile dysfunction in two mouse models of insulin resistance and obesity. Endocrinology 146, 5341-5349.

Bugger H, Chemnitius J-M & Doenst T. (2006). Differential changes in respiratory capacity and ischemia tolerance of isolated mitochondria from atrophied and hypertrophied hearts. Metabolism 55, 1097–1106.

Casale P, Devereux R, Milner M, Zullo G, Harshfield G, Pickering T & Laragh J. (1986). Value of echocardiographic measurement of left ventricular mass in predicting cardiovascular morbid events in hypertensive men. Ann Intern Med 105, 173-178.

Chien K. (1999). Stress pathways and heart failure. Cell 98, 555–558.

Chiu H, Kovacs A, Ford D, Hsu F, Garcia R, Herrero P, Saffitz J & Schaffer J. (2001). Novel mouse model of lipotoxic cardiomyopathy. J Clin Invest 107, 813-822.

Cohn J, Ferrari R & Sharpe N. (2000). Cardiac remodeling - concepts and clinical implications: a consensus paper from an international forum on cardiac remodeling. J Am Coll Cardiol 35, 569-582.

Corton J, Gillespie J & Hardie D. (1994). Role of the AMP-activated protein kinase in the cellular stress response. Curr Biol 4, 315–324.

Dabkowski E, Williamson C, Bukowski V, Chapman R, Leonard S, Peer C, Callery P & Hollander J. (2009). Diabetic cardiomyopathy-associated dysfunction in spatially distinct mitochondrial subpopulations. Am J Physiol Heart Circ Physiol 296, 359-369.

Davel A, Fukuda L, De Sá L, Munhoz C, Scavone C, Sanz-Rosa D, Cachofeiro V, Lahera V & Rossoni L. (2008). Effects of isoproterenol treatment for 7 days on inflammatory mediators in the rat aorta. Am J Physiol Heart Circ Physiol 295, 211-219.

De Silva D, Wilson R, Hutchinson C, Ip P, Garcia A, Lancel S, Ito M, Pimentel D & Sam F. (2009). Fenofibrate inhibits aldosterone-induced apoptosis in adult rat ventricular myocytes via stress-activated kinase-dependent mechanisms. Am J Physiol Heart Circ Physiol 296, 1983-1993.

Delerive P, De Bosscher K, Besnard S, Vanden Berghe W, Peters J, Gonzalez F, Fruchart J, Tedgui A, Haegeman G & Staels B. (1999). Peroxisome proliferator-activated receptor alpha negatively regulates the vascular inflammatory gene response by negative cross-talk with transcription factors NF-kappaB and AP-1. J Biol Chem 274, 32048-32054.

Delerive P, Fruchart C & Staels B. (2001). Peroxisome proliferator-activated receptors in inflammation control. J Endocrinol 169, 453–459.

Depre C, Shipley G, Chen W, Han Q, Doenst T, Moore M, Stepkowski S, Davies P & Taegtmeyer H. (1998). Unloaded heart in vivo replicates fetal gene expression of cardiac hypertrophy. Nat Med 4, 1269–1275.

Dhalla N, Temsah R & Netticadan T. (2000). Role of oxidative stress in cardiovascular diseases. J Hypertens 18, 655-673.

Dhalla N, Yates J, Lee S & Singh A. (1978). Functional and subcellular changes in the isolated rat heart perfused with oxidized isoproterenol. J Mol Cell Cardiol 10, 41.

Diep Q, Benkirane K, Amiri F, Cohn J, Endemann D & Schiffrin E. (2004). PPARalpha activator fenofibrate inhibits myocardial inflammation and fibrosis in angiotensin II-infused rats. J Mol Cell Cardiol 36, 295-304.

Ding B, Abe J, Wei H, Huang Q, Walsh R, Molina C, Zhao A, Sadoshima J, Blaxall B, Berk B & Yan C. (2005). Functional role of phosphodiesterase 3 in cardiomyocyte apoptosis: implication in heart failure. Circulation 111, 2469-2476.

Djouadi F, Brandt J, Weinheimer C, Leone T, Gonzalez F & Kelly D. (1999). The role of the peroxisome proliferator-activated receptor alpha (PPARα) in the control of cardiac lipid metabolism. Prostaglandins Leukot Essent Fatty Acids 60, 339–343.

Djouadi F, Weinheimer C, Saffitz J, Pitchford C, Bastin J, Gonzalez F & Kelly D. (1998). A gender-related defect in lipid metabolism and glucose homeostasis in peroxisome proliferator-activated receptor α-deficient mice. J Clin Invest 102, 1083–1091.

Duhaney T, Cui L, Rude M, Lebrasseur N, Ngoy S, De Silva D, Siwik D, Liao R & Sam F. (2007). Peroxisome proliferator-activated receptor -independent actions of fenofibrate exacerbates left ventricular dilation and fibrosis in chronic pressure overload. Hypertension 49, 1084–1094.

Dzau V, Hollenberg N & Williams G. (1983). Neurohumoral mechanism in heart failure: Role in pathogenesis, therapy and drug tolerance. Fed Proc 42, 3162-3169.

Eisenhofer G, Friberg P, Rundqvist B, Quyyumi A, Lambert G, Kaye D, Kopin I, Goldstein D & Esler M. (1996). Cardiac sympathetic nerve function in congestive heart failure. Circulation 93, 1667-1676.

Eliasson B. (2003). Cigarette smoking and diabetes. Progress in Cardiovascular Disease 45, 405-413.

Ergin A, Muntner P, Sherwin R, He J. (2004) Secular trends in cardiovascular disease mortality, incidence, and case fatality rates in adults in the United States. Am J Med 117, 219–227.

Feige J, Gelman L, Michalik L, Desvergne B & Wahli W. (2006). From molecular action to physiological outputs: peroxisome proliferatoractivated receptors are nuclear receptors at the crossroads of key cellular functions. Prog Lipid Res 45, 120-159.

Feng W & Li W. (2010). The study of ISO induced heart failure rat model. Exp Mol Pathol 88, 299-304.

Finck B & Kelly D. (2002). Peroxisome proliferator-activated receptor alpha signaling in the gene regulatory control of energy metabolism in the normal and diseased heart J Mol Cell Cardiol 34, 1249-1257.

Finck B, Lehman J, Leone T, Welch M, Bennett M, Kovacs A, Han X, Gross R, Kozak R, Lopaschuk G & Kelly D. (2002). The cardiac phenotype induced by PPAR-alpha overexpression mimics that caused by diabetes mellitus. J Clin Invest 109, 121-130.

Forcheron F, Basset A, Abdallah P, Del Carmine P, Gadot N & Beylot M. (2009). Diabetic cardiomyopathy: effects of fenofibrate and metformin in an experimental model--the Zucker diabetic rat. Cardiovasc Diabetol 24, 8-16.

Forman B, Chen J & Evans R. (1997). Hypolipidemic drugs, polyunsaturated fatty acids, and eicosanoids are ligands for peroxisome proliferator-activated receptors alpha and delta. Proc Natl Acad Sci USA 94 4312–4317

Fragasso G, Palloshi A, Puccetti P, Silipigni C, Rossodivita A, Pala M, Calori G, Alfieri O & Margonato A. (2006). A randomized clinical trial of trimetazidine, a partial free fatty acid oxidation inhibitor, in patients with heart failure. J Am Coll Cardiol 48, 992–998.

Francis G & Carlyle W. (1993). Hypothetical pathways of cardiac myocyte hypertrophy: response to myocardial injury. Eur Heart J 14, 49–56.

Francis G, Benedict C, Johnstone D, Kirlin P, Nicklas J, Liang C, Kubo S, Rudin-Toretsky E & Yusuf S. (1990). Comparison of neuroendocrine activation with left ventricular dysfunction with and without congestive heart failure. A substudy of the Studies of Left Ventricular Dysfunction (SOLVD). Circulation 82, 1724-1729.

Francis G, McDonald K & Cohn J. (1993). Neurohumoral activation in preclinical heart failure: remodeling and the potential for intervention. Circulation 87, 90–96.

Fried L, Shlipak M, Crump C, Bleyer A, Gottdiener J, Kronmal R, Kuller L & Newman A. (2003). Renal insufficiency as a predictor of cardiovascular outcomes and mortality in elderly individuals. JACC 41, 1364-1372.

Gao C, Sawicki G, Suarez-Pinzon W, Csont T, Wozniak M, Ferdinandy P & Schulz R. (2003). Matrix metalloproteinase-2 mediates cytokine-induced myocardial contractile dysfunction. Cardiovasc Res 57, 426-433.

Garnier A, Fortin D, Delomenie C, Momken I, Veksler V & Ventura-Clapier R. (2003). Depressed mitochondrial transcription factors and oxidative capacity in rat failing cardiac and skeletal muscles. J Physiol 551, 491–501.

Gauthier M, Miyoshi H, Souza S, Cacicedo J, Saha A, Greenberg A & Ruderman N. (2008). AMP-activated protein kinase is activated as a consequence of lipolysis in the adipocyte: potential mechanism and physiological relevance. J Biol Chem 283, 16514-16524.

Glatz J, Luiken J & Bonen A. (2001). Involvement of membrane-associated proteins in the acute regulation of cellular fatty acid uptake. J Mol Neurosci 16, 123-132.

Goldspink D, Burniston J, Ellison G, Clark W & Tan L-B. (2004). Catecholamine-induced apoptosis and necrosis in cardiac and skeletal myocytes of the rat in vivo: the same or separate death pathways? Exp Physiol 89, 407-416.

Goldspink D, Burniston J, Ellison G, Clark Wa & Tan L-B. (2004). Catecholamine-induced apoptosis and necrosis in cardiac and skeletal myocytes of the rat in vivo: the same or separate death pathways? Exp Physiol 89, 407-416.

Gopalakrishnan L & Scarpulla R. (1995). Structure, expression, and chromosomal assignment of the human gene encoding nuclear respiratory factor-1. J Biol Chem 270, 18019-18025.

Guellich A, Damy T, Lecarpentier Y, Conti M, Claes V, Samuel J, Quillard J, Hébert J, Pineau T & Coirault C. (2007). Role of oxidative stress in cardiac dysfunction of PPARalpha-/- mice. Am J Physiol Heart Circ Physiol 293, 93-102.

Gulick T, Cresci S, Caira T, Moore D & Kelly D. (1994). The peroxisome proliferator activated receptor regulates mitochondrial fatty acid oxidative enzyme gene expression. Proc Natl Acad Sci 91, 11012–11016.

Hansson A, Hance N, Dufour E, Rantanen A, Hultenby K, Clayton D, Wibom R & Larsson N. (2004). A switch in metabolism precedes increased mitochondrial biogenesis in respiratory chain-deficient mouse hearts. Proc Natl Acad Sci USA 101, 3136–3141.

Hasenfuss G. (1998). Animal models of human cardiovascular disease, heart failure and hypertrophy. Cardiovascular Research 39, 60 –76.

Havel R & Goldfien A. (1959). The role of the sympathetic nervous system in the metabolism of free fatty acids. J Lipid Res 1, 102-108.

Hawkins N, Wang D, McMurray J, Pfeffer M, Swedberg K, Granger C, Yusuf S, Pocock S, Ostergren J, Michelson E & Dunn F. (2007). Prevalence and prognostic implications of electrocardiographic left ventricular hypertrophy in heart failure: evidence from the CHARM programme. Heart 93, 59–64.

Heart Failure Society of America practice guidelines (HFSA) guidelines. (1999). HFSA guidelines for management of patients with heart failure caused by left ventricular systolic chamber dysfunction-pharmacological approaches. J Card Fail 5, 357-382.

Heather L, Catchpole A, Stuckey D, Cole M, Carr C & Clarke K. (2009). Isoproterenol induces in vivo functional and metabolic abnormalities: similar to those found in the infarcted rat heart. J Physiol Pharmacol 60, 31-39.

Hopkins T, Sugden M, Holness M, Kozak R, Dyck J & Lopaschuk G. (2003). Control of cardiac pyruvate dehydrogenase activity in peroxisome proliferator-activated receptor-alpha transgenic mice. Am J Physiol Heart Circ Physiol 285, 270–276.

Horman S, Browne G, Krause U, Patel J, Vertommen D, Bertrand L, Lavoinne A, Hue L, Proud C & Rider M. (2002). Activation of AMP-activated protein kinase leads to the phosphorylation of elongation factor 2 and an inhibition of protein synthesis. Curr Biol 12, 1419–1423.

Ibrahimim A, Sfeir Z, Magharaie H, Amri E, Grimaldi P & Abumrad N. (1996). Expression of the CD36 homolog FAT in fibroblast cells: Effects on fatty acid transport. Proc Natl Acad Sci USA 93, 2646–2651.

Ichihara S, Obata K, Yamada Y, Nagata K, Noda A, Ichihara G, Yamada A, Kato T, Izawa H, Murohara T & Yokota M. (2006). Attenuation of cardiac dysfunction by a PPAR-alpha agonist is associated with down-regulation of redox-regulated transcription factors. J Mol Cell Cardiol 41, 318-329.

Ichihara S, Yamada Y, Kawai Y, Osawa T, Furuhashi K, Duan Z & Ichihara G. (2007). Roles of oxidative stress and Akt signaling in doxorubicin cardiotoxicity. Biochem Biophys Res Commun 359, 27-33.

Ide T, Tsutsui H, Hayashidani S, Kang D, Suematsu N, Nakamura K, Utsumi H, Hamasaki N & Takeshita A. (2001). Mitochondrial DNA damage and dysfunction associated with oxidative stress in failing hearts after myocardial infarction. Circ Res 88, 529–535.

Iemitsu M, Miyauchi T, Maeda S, Tanabe T, Takanashi M, Irukayama-Tomobe Y, Sakai S, Ohmori H, Matsuda M & Yamaguchi I. (2002). Aging-induced decrease in the PPAR-alpha level in hearts is improved by exercise training. Am J Physiol Heart Circ Physiol 283, 1750–1760.

Ikeuchi M, Matsusaka H, Kang D, Matsushima S, Ide T, Kubota T, Fujiwara T, Hamasaki N, Takeshita A, Sunagawa K & Tsutsui H. (2005). Overexpression of mitochondrial transcription factor a ameliorates mitochondrial deficiencies and cardiac failure after myocardial infarction. Circulation 112, 683-690.

Ingwall J & Weiss R. (2004). Is the failing heart energy starved?: on using chemical energy to support cardiac function. Circ Res 95, 135–145.

Iribarrenet C, Karter A, Go A, Ferrara A, Liu J, Sidney S & Selby J. (2001). Glycemic control and heart failure among adult patients with diabetes. Circulation 103, 2668-2673.

Irukayama-Tomobe Y, Miyauchi T, Kasuya Y, Sakai S, Goto K & Yamaguchi I. (2004). Activation of peroxisome proliferator-activated receptor-alpha decreases endothelin-1-induced p38 mitogen-activated protein kinase activation in cardiomyocytes. J Cardiovasc Pharmacol 44, 358-361.

Izquierdo J, Ricart J, Ostronoff L, Egea G & Cuezva J. (1995). Changing patterns of transcriptional and post-transcriptional control of β-F1-ATPase gene expression during mitochondrial biogenesis in liver. J Biol Chem 270, 10342–10350.

Javadov S, Huang C, Kirshenbaum L & Karmazyn M. (2005). NHE-1 inhibition improves impaired mitochondrial permeability transition and respiratory function during postinfarction remodelling in the rat. J Mol Cell Cardiol 38, 135–143.

Javadov S, Purdham D, Zeidan A & Karmazyn M. (2006). NHE-1 inhibition improves cardiac mitochondrial function through regulation of mitochondrial biogenesis during postinfarction remodeling. Am J Physiol Heart Circ Physiol 291, 1722-1730.

Jin Y, Hasebe N, Matsusaka T, Natori S, Ohta T, Tsuji S & Kikuchi K. (2007). Magnesium attenuates isoproterenol-induced acute cardiac dysfunction and beta-adrenergic desensitization. Am J Physiol Heart Circ Physiol 292, 1593-1599.

Juenger J, Schellberg D, Kraemer S, Haunstetter A, Zugck C, Herzog W & Haass M. (2002). Health related quality of life in patients with congestive heart failure: comparison with other chronic diseases and relation to functional variables. Heart 87, 235-241.

Kahn B, Alquier T, Carling D, Hardie D & King K. (2005). AMP-activated protein kinase: ancient energy gauge provides clues to modern understanding of metabolism. Cell Metabolism 1, 15–25.

Kalsi K, Smolenski R, Pritchard R, Khaghani A, Seymour A & Yacoub M. (1999). Energetics and function of the failing human heart with dilated or hypertrophic cardiomyopathy. Eur J Clin Invest 29, 469–477.

Kamerman P, Modisa B & Mphahlele N. (2004). Atorvastatin, a potent HMG-CoA reductase inhibitor, is not antipyretic in rats. J Therm Biol 29, 431–435.

Kang D, Kim S & Hamasaki N. (2007). Mitochondrial transcription factor A (TFAM): roles in maintenance of mtDNA and cellular functions. Mitochondrion 7, 39-44.

Karbowska J, Kochan Z & Smolenski R. (2003). Peroxisome proliferator-activated receptor alpha is downregulated in the failing human heart. Cell Mol Biol Lett 8, 49–53.

Kelly D & Scarpulla R. (2004). Transcriptional regulatory circuits controlling mitochondrial biogenesis and function. Genes Dev 18, 357–368.

Kelly D, Gordon J, Alpers R & Strauss A. (1989). The tissue-specific expression and developmental regulation of the two nuclear genes encoding rat mitochondrial proteins. Medium-chain acyl-CoA dehydrogenase and mitochondrial malate dehydrogenase. J Biol Chem 264, 921–925.

Kenchaiah S, Narula J & Vasan R. (2004). Impact of obesity on the risk of heart failure and survival after the onset of heart failure. Med Clin North Am 88, 1273-1294.

Kerner J & Hoppel C. (2000). Fatty acid import into mitochondria. Biochim Biophys Acta 1486, 1–17.

Kim S, Zhao Z, Lee Y, Lee K, Kang S, Choi D, Lim S, Chung N, Lee H & Cha B. (2003). Left-ventricular diastolic dysfunction may be prevented by chronic treatment with PPAR-alpha or -gamma agonists in a type 2 diabetic animal model. Diabetes Metab Res Rev 19, 487-493.

Koh H, Hirshman M, He H, Li Y, Manabe Y, Balschi J & Goodyear L. (2007). Adrenaline is a critical mediator of acute exercise-induced AMP-activated protein kinase activation in adipocytes. Biochem J 403, 473-481.

Kong J & Rabkin S. (2004). Reduction of palmitate-induced cardiac apoptosis by fenofibrate. Mol Cell Biochem 258, 1-13.

Koren M, Devereux R, Casale P, Savage D & Laragh J. (1991). Relation of left ventricular mass and geometry to morbidity and mortality in uncomplicated essential hypertension. Ann Intern Med 114, 345-352.

Kudo N, Barr A, Desai S & Lopaschuk G. (1995). High rates of fatty acid oxidation during reperfusion of ischemic hearts are associated with a decrease in malonyl-coA levels due to an increase in AMPK inhibition of acetyl-CoA carboxylase. J Biol Chem 270, 17513-17520.

Labinskyy V, Bellomo M, Chandler M, Young M, Lionetti V, Qanud K, Bigazzi F, Sampietro T, Stanley W & Recchia F. (2007). Chronic activation of peroxisome proliferator-activated receptor-alpha with fenofibrate prevents alterations in cardiac metabolic phenotype without changing the onset of decompensation in pacing-induced heart failure. J Pharmacol Exp Ther 321, 165-171.

Larkin J, Frank B, Gaspard R, Duka I, Gavras H & Quackenbush J. (2004). Cardiac transcriptional response to acute and chronic angiotensin II treatments. Physiol Genomics 18, 152-166.

Larsson N, Wang J, Wilhelmsson H, Oldfors A, Rustin P, Lewandoski M, Barsh G & Clayton D. (1998). Mitochondrial transcription factor A is necessary for mtDNA maintenance and embryogenesis in mice. Nat Genet 18, 231–236.

Lavie C, Ventura H & Messerli F. (1988). Cardiomyopathy of obesity. Int Med Spec 9, 57-71.

Lavie C, Ventura H & Messerli F. (1992). Left ventricular hypertrophy: its relationship to obesity and hypertension. Postgrad Med 91, 131-143

LeBrasseur N, Duhaney T-A, De Silva D, Cui L, Ip P, Joseph L & Sam F. (2007). Effects of fenofibrate on cardiac remodeling in aldosterone-induced hypertension. Hypertension 50, 489-496.

Lee L, Campbell R, Scheuermann-Freestone M, Taylor R, Gunaruwan P, Williams L, Ashrafian H, Horowitz J, Fraser A, Clarke K & Frenneaux M. (2005). Metabolic modulation with perhexiline in chronic heart failure: a randomized, controlled trial on short-term use of a novel treatment. Circulation 112, 3280 –3288.

Lee M, Gardin J, Lynch J, Smith V, Tracy R, Savage P, Szklo M & Ward B. (1997). Diabetes mellitus and echocardiographic left ventricular function in free-living elderly men and women: the Cardiovascular Health Study. Am Heart J 133, 36-43.

Lee S, Pineau T, Drago J, Lee E, Owens J, Kroetz D, Fernandez-Salguero P, Westphal H & Gonzalez F (1995). Targeted disruption of the α isoform of the peroxisome proliferator-activated receptor gene in mice results in abolishment of the pleiotropic effects of peroxisome proliferators. Mol Cell Biol 15, 3012–3022.

Lee WJ, Kim M, Park HS, Kim HS, Jeon MJ, Oh KS, Koh EH, Won JC, Kim MS, Oh GT, Yoon M, Lee KU & Park JY. (2006). AMPK activation increases fatty acid oxidation in skeletal muscle by activating PPARalpha and PGC-1. Biochem Biophys Res Commun 340(1), 291-295.

Lehman J & Kelly D. (2002). Transcriptional activation of energy metabolic switches in the developing and hypertrophied heart. Clin Exp Pharmacol Physiol 29, 339–345.

Lehman J, Barger P, Kovacs A, Saffitz J, Medeiros D & Kelly D. (2000). Peroxisome proliferator-activated receptor gamma coactivator-1 promotes cardiac mitochondrial biogenesis. J Clin Invest 106, 847–856.

Lei B, Lionetti V, Young M, Chandler M, d'Agostino C, Kang E, Altarejos M, Matsuo K, Hintze T, Stanley W & Recchia F. (2004). Paradoxical downregulation of the glucose oxidation pathway despite enhanced flux in severe heart failure. J Mol Cell Cardiol 36, 567–576.

Levy D, Garrison R, Savage D, Kannel W & Castelli W. (1990). Prognostic implications of echocardiographically determined left ventricular mass in the Framingham Heart Study. N Engl J Med 322, 1561-1566.

Levy D, Larson M, Vasan R, Kannel W & Ho K. (1996). The progressions from hypertension to congestive heart failure. JAMA 275, 1557-1562.

Liang F, Wang F, Zhang S & Gardner D. (2003). Peroxisome proliferator activated receptor (PPAR)alpha agonists inhibit hypertrophy of neonatal rat cardiac myocytes. Endocrinology 144, 4187-4194.

Liangpunsakul S, Wou S, Wineinger K, Zeng Y, Cyganek I, Jayaram H & Crabb D. (2009). Effects of WY-14,643 on the phosphorylation and activation of AMP-dependent protein kinase. Arch Biochem Biophys 485, 10-15.

Lionetti V, Linke A, Chandler M, Young M, Penn M, Gupte S, d'Agostino C, Hintze T, Stanley W & Recchia F. (2005). Carnitine palmitoyl transferase-I inhibition prevents ventricular remodeling and delays decompensation in pacing-induced heart failure. Cardiovasc Res 66, 274–281.

Listenberger L & Schaffer J. (2002). Mechanisms of lipoapoptosis: implications for human heart disease. Trends Cardiovasc Med 12, 134–138.

Liu Y-H, Carretero O, Cingolani O, Liao T-D, Sun Y, Xu J, Li L, Pagano P, Yang J & Yang X-P. (2005). Role of inducible nitric oxide synthase in cardiac function and remodeling in mice with heart failure due to myocardial infarction. Am J Physiol Heart Circ Physiol 289, 2616–2623.

Lopaschuk G, Belke D, Gamble J, Itoi T & Schonekess B. (1994). Regulation of fatty acid oxidation in the mammalian heart in health and disease. Biochim Biophys Acta 1213, 263–276.

Luiken J, Coort S, Willems J, Coumans W, Bonen A, van der Vusse G & Glatz J. (2003). Contraction-induced fatty acid translocase/CD36 translocation in rat cardiac myocytes is mediated through AMP-activated protein kinase signaling. Diabetes Care 52, 1627–1634.

Mangelsdorf D & Evans R. (1995). The RXR heterodimers and orphan receptors. Cell 83, 841–850.

Mann D & Young J. (1994). Basic mechanisms in congestive heart failure: Recognizing the role of proinflammatory cytokines. Chest 105, 897-904.

Marra G, Cotroneo P, Pitocco D, Manto A, Di Leo M, Ruotolo V, Caputo S, Giardina B, Ghirlanda G& Santini S. (2002). Early increase of oxidative stress and reduced antioxidant defenses in patients with uncomplicated type 1 diabetes: a case for gender difference. Diabetes Care 25, 370–375.

Mohan P & Bloom S. (1999). Lipolysis is an important determinant of isoproterenol-induced myocardial necrosis. Cardiovasc Pathol 8, 255-261.

Morgan E, Chandler M, Young M, McElfresh T, Kung T & Rennison J. (2006). Dissociation between gene and protein expression of metabolic enzymes in a rodent model of heart failure. Eur J Heart Fail 8, 687–693.

Morgan E, Rennison J, Young M, McElfresh T, Kung T, Tserng K, Hoit B, Stanley W & Chandler M. (2005). Effects of chronic activation of peroxisome proliferator-activated receptor alpha or high-fat feeding in a rat infarct model of heart failure. Am J Physiol Heart Circ Physiol 290, 1899–1904.

Motojima K, Passilly P, Peters J, Gonzalez F & Latruffe N. (1998). Expression of putative fatty acid transporter genes are regulated by peroxisome proliferator-activated receptor alpha and gamma activators in a tissue and inducer-specific manner. J Biol Chem 273, 710-714.

Mudd J & Kass D. (2008). Tackling heart failure in the twenty-first century. Nature 451, 919-928.

Murakami H, Murakami R, Kambe F, Cao X, Takahashi R, Asai T, Hirai T, Numaguchi Y, Okumura K, Seo H & Murohara T. (2006). Fenofibrate activates AMPK and increases eNOS phosphorylation in HUVEC. Biochem Biophys Res Commun 341, 973-978.

Murray A, Cole M, Lygate C, Carr C, Stuckey D, Little S, Neubauer S & Clarke K. (2008). Increased mitochondrial uncoupling proteins, respiratory uncoupling and decreased efficiency in the chronically infarcted rat heart. J Mol Cell Cardiol 44, 694–700.

Murray D, Prabhu S & Chandrasekar B. (2000). Chronic beta-adrenergic stimulation induces myocardial proinflammatory cytokine expression. Circulation 101, 2338-2341.

Murray R, Granner D, Mayes P & Rodwell V. (2003). Harper's Illustrated Biochemistry. Lange Medical Books/ MgGraw Hill, New York, NY.

Nakamura R, Egashira K, Machida Y, Hayashidani S, Takeya M, Utsumi H & refs) eatfo. (2002). Probucol attenuates left ventricular dysfunction and remodelling in tachycardia-induced heart failure: roles of oxidative stress and inflammation. Circulation 106, 362–367.

Narula J, Haider N, Virmani R, DiSalvo T, Kolodgie F, Hajjar R, Schmidt U, Semigran M, Dec G & Khaw B. (1996). Apoptosis in myocytes in end-stage heart failure. N Engl J Med 335, 1182–1189.

Neglia D, De Caterina A, Marraccini P, Natali A, Ciardetti M, Gastaldelli A, Ciociaro D, Pellegrini P, Testa R, Menichetti L, L'Abbate A, Stanley W & Recchia F. (2007). Impaired myocardial metabolic reserve and substrate selection flexibility during stress in patients with idiopathic dilated cardiomyopathy. Am J Physiol Heart Circ Physiol 293, 3270-3278.

Neubauer S. (2007). The failing heart—an engine out of fuel. N Engl J Med 356, 1140–1115.

Nishikawa T, Edelstein D, Du X, Yamagishi S, Matsumura T, Kaneda Y, Yorek M, Beebe D, Oates P, Hammes H, Giardino I & Brownlee M. (2000). Normalizing mitochondrial superoxide production blocks three pathways of hyperglycaemic damage. Nature 404, 787-790.

Norton G, Woodiwiss A, Gaasch W, Mela T, Chung E & Aurigemma G. (2002). Heart failure in pressure overload hypertrophy: The relative roles of ventricular remodeling and myocardial dysfunction. J Am Coll Cardiol 39, 664-671.

Ogata T, Miyauchi T, Sakai S, Irukayama-Tomobe Y, Goto K & Yamaguchi I. (2002). Stimulation of peroxisome proliferators-activated receptor alpha (PPAR-alpha) attenuates

cardiac fibrosis and endothelin-1 production in pressure-overloaded rat hearts. Clin Sci 103, 284–288.

Ogata T, Miyauchi T, Sakai S, Takanashi M, Irukayama-Tomobe Y & Yamaguchi I. (2004). Myocardial fibrosis and diastolic dysfunction in deoxycorticosterone acetate-salt hypertensive rats is ameliorated by the peroxisome proliferator-activated receptor-alpha activator fenofibrate, partly by suppressing inflammatory responses associated with the nuclear factor-kappa-B pathway. J Am Coll Cardiol 43, 1481-1488.

Opie L, Commerford P, Gersh B & Pfeffer M. (2006). Controversies in ventricular remodelling. Lancet 367, 356-367.

Osadchii O, Norton G, McKechnie R, Deftereos D & Woodiwiss A. (2007). Cardiac dilatation and pump dysfunction without intrinsic myocardial systolic failure following chronic beta-adrenoreceptor activation. Am J Physiol Heart Circ Physiol, 1898-1905.

Osadchii O, Woodiwiss A, Alves N & Norton G. (2005). Mechanisms of preserved baseline cardiac systolic function in rats with adrenergic inotropic downregulation. Life Sci 78:366–375.

Osorio J, Stanley W, Linke A, Castellari M, Diep Q, Panchal A, Hintze T, Lopaschuk G & Recchia F. (2002). Impaired myocardial fatty acid oxidation and reduced protein expression of retinoid X receptor-alpha in pacing-induced heart failure. Circulation 106, 606–612.

Parker M. (1992). The neurohormonal hypothesis: a theory to explain the mechanism of disease progression in heart failure. J AM Coll Cardiol 20, 248-254.

Pearce R. (1906). Experimental myocarditis: a study of the histological changes following intravenous injections of adrenaline. J Exp Med 8, 400.

Pfeffer M & Braunwald E. (1990). Ventricular remodeling after myocardial infarction: experimental observations and clinical implications. Circulation 81, 1161–1172.

Ponticos M, Lu Q, Morgan J, Hardie D & Partridge T. (1998). Dual regulation of the AMP-activated protein kinase provides a novel mechanism for the control of creatine kinase in skeletal muscle. EMBO J 17, 1688-1699.

Qin F, Shite J, Mao W & Liang C. (2003). Selegiline attenuates cardiac oxidative stress and apoptosis in heart failure: association with improvement of cardiac function. Eur J Pharmacol 461, 149–158.

Rajadurai M & Prince P. (2007). Preventive effect of naringin on cardiac mitochondrial enzymes during isoproterenol-induced myocardial infarction in rats: a transmission electron microscopic study. J Biochem Mol Toxicol 21, 354-361.

Recchia F, McConnell P, Bernstein R, Vogel T, Xu X & Hintze T. (1998). Reduced nitric oxide production and altered myocardial metabolism during the decompensation of pacing-induced heart failure in the conscious dog. Circ Res 83, 969–979.

Remondino A, Rosenblatt-Velin N, Montessuit C, Tardy I, Papageorgiou I & Dorsaz P. (2000). Altered expression of proteins of metabolic regulation during remodeling of the left ventricle after myocardial infarction. J Mol Cell Cardiol 32, 2025–2034.

Roger V, Weston S, Redfield M, Hellermann-Homan J, Killian J, Yawn B & Jacobsen S. (2004). Trends in heart failure incidence and survival in a community-based population. JAMA 292, 344-350.

Rosenblatt-Velin N, Montessuit C, Papageorgiou I, Terrand J & Lerch R. (2001). Postinfarction heart failure in rats is associated with upregulation of GLUT-1 and downregulation of genes of fatty acid metabolism. Cardiovasc Res 52, 407–416.

Ruderman N, Saha A, Vavvas D & Witters L. (1999). Malonyl-CoA, fuel sensing, and insulin resistance. Am J Physiol Endocrinol Metab 276, 1–18.

Russell L, Mansfield C, Lehman J, Kovacs A, Courtois M, Saffitz J, Medeiros D, Valencik M, McDonald J & Kelly D. (2004). Cardiac-specific induction of the transcriptional coactivator peroxisome proliferator-activated receptor gamma coactivator-1alpha promotes mitochondrial biogenesis and reversible cardiomyopathy in a developmental stage-dependent manner. Circ Res 94, 525–533 (a).

Russell R, 3rd. , Li J, Coven D, Pypaert M, Zechner C, Palmeri M, Giordano F, Mu J, Birnbaum M & Young L. (2004). AMP-activated protein kinase mediates ischemic glucose uptake and prevents postischemic cardiac dysfunction, apoptosis, and injury. J Clin Invest 114, 495–503 (b).

Sabbah H, Sharov V, Riddle J, Kono T, Lesch M & Goldstein S. (1992). Mitochondrial abnormalities in myocardium of dogs with chronic heart failure. J Mol Cell Cardiol 24, 1333-1347.

Sabbah H, Stanley W, Sharov V, Mishima T, Tanimura M, Benedict C, Hegde S & Goldstein S. (2000). Effects of dopamine beta-hydroxylase inhibition with nepicastat on the progression of left ventricular dysfunction and remodeling in dogs with chronic heart failure. Circulation 102, 1990–1995.

Sahn D, DeMaria A, Kisslo J & Weyman A. (1978). Recommendations regarding quantitation in M-mode echocardiography: results of a survey of echocardiographic measurements. Circulation 58, 1072-1083.

Salt I, Celler J, Hawley S, Prescott A & Woods A. (1998). AMP-activated protein kinase: greater AMP dependence, and preferential nuclear localization, of complexes containing alpha2 isoform. Biochem J 334, 177-187.

Sambandam N, Morabito D, Wagg C, Finck B, Kelly D & Lopaschuk G. (2006). Chronic activation of PPARalpha is detrimental to cardiac recovery after ischemia. Am J Physiol Heart Circ Physiol 290, 87-95.

Sanbe A, Tanonaka K, Kobayasi R & Takeo S. (1995). Effects of long-term therapy with ACE inhibitors, captopril, enalapril and trandolapril, on myocardial energy metabolism in rats with heart failure following myocardial infarction. J Mol Cell Cardiol 27, 2209–2222.

Sasaki H, Asanuma H, Fujita M, Takahama H, Wakeno M, Ito S, Ogai A, Asakura M, Kim J, Minamino T, Takashima S, Sanada S, Sugimachi M, Komamura K, Mochizuki N & Kitakaze M. (2009). Metformin prevents progression of heart failure in dogs: role of AMP-activated protein kinase. Circulation 119, 2568-2577.

Schaffer J. (2002). Fatty acid transport: the roads taken. Am J Physiol Endocrinol Metab 282, E239–E246.

Schaffer J. (2003). Lipotoxicity: when tissues overeat. Curr Opin Lipidol 14, 281-287.

Schaper J, Froede R, Hein St Buck A, Hashizume H, Speiser B, Friedl A & Bleese N. (1991). Impairment of the myocardial ultrastructure and changes of the cytoskeleton in dilated cardiomyopathy. Circulation 83, 504–514.

Scheubel R, Tostlebe M, Simm A, Rohrbach S, Prondzinsky R, Gellerich F, Silber R-E & Holtz J. (2002). Dysfunction of mitochondrial respiratory chain complex I in human failing myocardium is not due to disturbed mitochondrial gene expression. J Am Coll Cardiol 40, 2174–2181.

Schillaci G, Verdecchia P, Porcellati C, Cuccurullo O, Cosco C & Perticone F. (2000). Continuous relation between left ventricular mass and cardiovascular risk in essential hypertension. Hypertension 35, 580–586.

Schocken D, Benjamin E, Fonarow G, Krumholz H, Levy D, Mensah G, Narula J, Shor E, Young J & Hong Y. (2008). Prevention of heart failure: A scientific statement from the American Heart Association Councils on Epidemiology and Prevention, Clinical Cardiology, Cardiovascular Nursing, and High Blood Pressure Research; Quality of Care and Outcomes Research Interdisciplinary Working Group; and Functional Genomics and Translational Biology Interdisciplinary Working Group. Circulation 117, 2544-2565.

Schulz H. (1994). Regulation of fatty acid oxidation in heart. J Nutr 124, 165–171.

Seymour A. (2003). Mitochondrial function—a limiting factor in heart failure?. In Pathophysiology of cardiovascular disease, 1 edn, ed. Dhalla N & Rupp H, pp. 23–33. Kluwer academic publishers, Boston.

Shen W, Asai K, Uechi M, Mathier M, Shannon R & Vatner S. (1999). Progressive loss of myocardial ATP due to a loss of total purines during the development of heart failure in dogs: a compensatory role for the parallel loss of creatine. Circulation 100, 2113–2118.

Shibata R, Ouchi N, Ito M, Kihara S, Shiojima I, Pimentel D, Kumada M, Sato K, Schiekofer S, Ohashi K, Funahashi T, Colucci W & Walsh K. (2004). Adiponectin-mediated modulation of hypertrophic signals in the heart. Nat Med 10, 1384–1389.

Shizukuda Y, Buttrick P, Geenen D, Borczuk AK, RN. & Sonnenblick E. (1998). Beta-adrenergic stimulation causes cardiocyte apoptosis: innfluence of tachycardia and hypertrophy. Am J Physiol Heart Circ Physiol 275, 961-968.

Sidhu J, Rajawat Y, Rami T, Gollob M, Wang Z, Yuan R, Marian A, DeMayo F, Weilbacher D, Taffet G, Davies J, Carling D, Khoury D & Roberts R. (2005). Transgenic mouse model of ventricular preexcitation and atrioventricular reentrant tachycardia induced by an AMP-activated protein kinase loss-of-function mutation responsible for Wolff-Parkinson-White syndrome. Circulation 111, 21–29.

Singh K, Xiao L, Remondino A, Sawyer D & Colucci W. (2001). Adrenergic regulation of cardiac myocytes apoptosis. J Cell Physiol 189, 257-265.

Smeets P, de Vogel-van den Bosch H, Willemsen P, Stassen A, Ayoubi T, van der Vusse G & van Bilsen M. (2008). Transcriptomic analysis of PPARalpha-dependent alterations during cardiac hypertrophy. Physiol Genomics 36, 15-23(b).

Smeets P, Teunissen B, Planavila A, de Vogel-van den Bosch H, Willemsen P, van der Vusse G & van Bilsen M. (2008). Inflammatory pathways are activated during cardiomyocyte

hypertrophy and attenuated by peroxisome proliferator-activated receptors PPARalpha and PPARdelta. J Biol Chem 283, 29109-29118(a).

Stryler L. (1999). Biochemistry. WH Freeman and Company, New York.

Stuck B, Lenski M, Bohm M & Laufs U. (2008). Metabolic switch and hypertrophy of cardiomyocytes following treatment with angiotensin II are prevented by AMP-activated protein kinase. J Biol Chem 283, 32562-32569.

Studies of Left Ventricular Dysfunction (SOLVD) Investigators. (1992). Effect of enalapril on mortality and the development of heart failure in asymptomatic patients with reduced left ventricular ejection fractions. N Engl J Med 327, 685–691.

Suarez J, Hu Y, Makino A, Fricovsky E, Wang H & Dillmann W. (2008). Alterations in mitochondrial function and cytosolic calcium induced by hyperglycemia are restored by mitochondrial transcription factor A in cardiomyocytes. Am J Physiol Cell Physiol 295, 1561-1568.

Suchalatha S & Shyamala-Devi C. (2004). Effect of Arogh-a polyherbalformulation on the marker enzymes in isoproterenol-induced myocardial injury. Indian J Clin Biochem 19, 184-189.

Suga H. (1990). Ventricular energetics. Physiol Rev 70, 247–277.

Sugden P & Clerk A. (1998). Cellular mechanisms of cardiac hypertrophy. J Mol Med 76, 725-746.

Taegtmeyer H. (2002). Switching metabolic genes to build a better heart. Circulation 106, 2125-31.

Tang W & Francis G. (2003). Novel pharmacological treatments for heart failure. Expert Opin Invest Drugs 12, 1791–1801.

Taylor M, Wallhaus T, Degrado T, Russell D, Stanko P, Nickles R & Stone C. (2001). An evaluation of myocardial fatty acid and glucose uptake using PET with [18F]fluoro-6-thia-heptadecanoic acid and [18F]FDG in Patients with Congestive Heart Failure. J Nucl Med 42, 55–62.

Teerlink J, Pfeffer J & Pfeffer M. (1994). Progressive ventricular remodeling in response to diffuse isoproterenol-induced myocardial necrosis in rats. Circ Res 75, 105–113.

Tian R, Musi N, D'Agostino J, Hirshman M & Goodyear L. (2001). Increased adenosine monophosphate-activated protein kinase activity in rat hearts with pressure-overload hypertrophy. Circulation 104, 1664 –1669.

Van Bilsen M, Smeets P, Gilde A & van der Vusse G. (2004). Metabolic remodelling of the failing heart: the cardiac burn-out syndrome? Cardiovasc Res 61, 218-226.

Van Bilsen M, Van Nieuwenhoven F & Van der Vusse G. (2009). Metabolic remodelling of the failing heart: beneficial or detrimental? Cardiovasc Res 81, 420-428.

Van Dam P, Van Asbeck B, Erkelens D, Marx J, Gispen W & Bravenboer B. (1995). The role of oxidative stress in neuropathy and other diabetic complications. Diabetes Metab Rev 11, 181–192.

Van den Bosch B, Lindsey P, van den Burg C, van der Vlies S, Lips D, van der Vusse G, Ayoubi T, Doevendans P & Smeets H. (2006). Early and transient gene expression changes in pressure overload-induced cardiac hypertrophy in mice. Genomics 88, 480–488.

Van der Lee K, Vork M, de Vries Jea, Willemsen H, Glatz J, Reneman R, Van der Vusse G & Van Bilsen M. (2000). Long-chain fatty acid-induced changes in gene expression in neonatal cardiac myocytes. J Lipid Res 41, 41–47.

Van der Vusse G, van Bilsen M & Glatz J. (2000). Cardiac fatty acid uptake and transport in health and disease. Cardiovasc Res 45, 279–293.

Van Vleet J, Ferrans J & Herman E. (2002). Cardiovascular and skeletal muscle system. In Handbook of Toxicologic Pathology, ed. Haschek W, pp. 363–455. Academic Press, San Diego, CA, USA.

Vaughan M. (1962). The production and release of glycerol by adipose tissue incubated in vitro. J Biol Chem 237, 3354-3358.

Vega R, Huss J & Kelly D. (2000). The coactivator PGC-1 cooperates with peroxisome proliferator-activated receptor in transcriptional control of nuclear genes encoding mitochondrial fatty acid oxidation enzymes. Mol Cell Biol 20, 1868–1876.

Verreth W, Ganame J, Mertens A, Bernar H, Herregods M & Holvoet P. (2006). Peroxisome proliferator-activated receptor-α, γ-agonist improves insulin sensitivity and prevents loss of left ventricular function in obese dyslipidemic mice. Arterioscler Thromb Vasc Biol 26, 922–928.

Walsh C, Larson M, Evans J, Djousse L, Ellison R, Vasan R & Levy D. (2002). Alcohol consumption and risk for congestive heart failure in the Framingham Study. Ann Intern Med 136, 181-191.

Wang J, Wilhelmsson H, Graff C, Li H, Oldfors A, Rustin P, Bruning J, Kahn C, Clayton D, Barsh G, Thoren P & Larsson N. (1999). Dilated cardiomyopathy and atrioventricular

conduction blocks induced by heartspecific inactivation of mitochondrial DNA gene expression. Nat Genet 21, 133–137.

Weber K. (1997). Extracellular matrix remodeling in heart failure: a role for de novo angiotensin II generation. Circulation 96, 4065–4082.

Winder W, Holmes B, Rubink D, Jensen E, Chen M & Holloszy J. (2000). Activation of AMP-activated protein kinase increases mitochondrial enzymes in skeletal muscle. J Appl Physiol 88, 2219-2226.

Wisneski J, Gertz E, Neese R, Gruenke L, Morris D & Craig J. (1985). Metabolic fate of extracted glucose in normal human myocardium. J Clin Invest 76, 1819–1827.

Woodiwiss A, Tsotetsi O, Sprott S, Lancaster E, Mela T, Chung E, Meyer T & Norton G. (2001). Reduction in myocardial collagen cross-linking parallels left ventricular dilatation in rat models of systolic chamber dysfunction. Circulation 103, 155-160.

Wu Q, Tang Q, Xiao Q, Wu P, Gao A & Li L. (2010). PPARalpha agonist prevented the apoptosis induced by glucose and fatty acid in neonatal cardiomyocytes. J Endocrinol Invest Mar 30,[Epub ahead of print].

Wu Z, Puigserver P, Andersson U, Zhang C, Adelmant G, Mootha V, Troy A, Cinti S, Lowell B, Scarpulla R & Spiegelman B. (1999). Mechanisms controlling mitochondrial biogenesis and respiration through the thermogenic coactivator PGC-1. Cell 98, 115–124.

Xia Y, Buja L, Scarpulla R & McMillin J. (1997). Electrical stimulation of neonatal cardiomyocytes results in the sequential activation of nuclear genes governing mitochondrial proliferation and differentiation. Proc Natl Acad Sci USA 94, 11399–11404.

Xu S, Zhong M, Zhang L, Wang Y, Zhou Z, Hao Y, Zhang W, Yang X, Wei A, Pei L & Yu Z. (2009). Overexpression of Tfam protects mitochondria against beta-amyloid-induced oxidative damage in SH-SY5Y cells. FEBS J 276, 3800-3809.

Xu Y, Lu L, Greyson C, Rizeq M, Nunley K, Wyatt B, Bristow M, Long C & Schwartz G. (2006). The PPAR-{alpha} activator fenofibrate fails to provide myocardial protection in ischemia and reperfusion in pigs. Am J Physiol Heart Circ Physiol 290, 1798-1807.

Yamagishi S, Edelstein D, Du X, Kaneda Y, Guzman M & Brownlee M. (2001). Leptin induces mitochondrial superoxide production and monocyte chemoattractant protein-1 expression in aortic endothelial cells by increasing fatty acid oxidation via protein kinase. A J Biol Chem 276, 25096–25100.

Yamaguchi S, Katahira H, Ozawa S, Nakamichi Y, Tanaka T, Shimoyama T, Takahashi K, Yoshimoto K, Imaizumi M, Nagamatsu S & Ishida H. (2005). Activators of AMP-activated protein kinase enhance GLUT4 translocation and its glucose transport activity in 3T3-L1 adipocytes. Am J Physiol Endocrinol Metab 289, 643-649.

Yan J, Young M, Cui L, Lopaschuk G, Liao R & Tian R. (2009). Increased glucose uptake and oxidation in mouse hearts prevent high fatty acid oxidation but cause cardiac dysfunction in diet-induced obesity. Circulation 119, 2818-2828.

Yeh C, Chen T, Lee C, Wu Y, Lin Y & Lin P. (2006). Cardiomyocytic apoptosis following global cardiac ischemia and reperfusion can be attenuated by peroxisome proliferator-activated receptor alpha but not gamma activators. Shock 26, 262-270.

Yogeeta S, Raghavendran H, Gnanapragasam A, Subhashini R & Devaki T. (2006). Ferulic acid with ascorbic acid synergistically extenuates the mitochondrial dysfunction during beta-adrenergic catecholamine induced cardiotoxicity in rats. Chem Biol Interact 163, 160-169.

Yokoham T, Vaca L, Rosen R, Durante W, Hazarika P & Mann D. (1993). Cellular basis for the negative inotropic effects of tumour necrosis factor alpha in the adult mammalian heart. J Clin Invest 92, 2303-2312.

Young L, Li J, Baron S & Russell R. (2005). AMP-activated protein kinase: a key stress signaling pathway in the heart. Trends Cardiovasc Med 15, 110–118.

Young M, Laws F, Goodwin G & Taegtmeyer H. (2001). Reactivation of peroxisome proliferator-activated receptor alpha is associated with contractile dysfunction in hypertrophied rat heart. J Biol Chem 276, 44390–44395.

Yuan J, Wu J & Han Z. (2008). Fenofibrate improves energy metabolism and attenuates isoproterenol induced acute myocardial ischemic injury in rats via PPAR alpha activation. honghua Xin Xue Guan Bing Za Zhi 36, 847-850.

Zarrinpashneh E, Beauloye C, Ginion A, Pouleur A, Havaux X, Hue L, Viollet B, Vanoverschelde J & Bertrand L. (2008). AMPKalpha2 counteracts the development of cardiac hypertrophy induced by isoproterenol. Biochem Biophys Res Commun 376, 677-681.

Zhang G, Kimura S, .N, ishiyama A, Shokoji T, Rahman M, Yao L, Nagai Y, Fujisawa Y, Miyatake A & Abe Y. (2005). Cardiac oxidative stress in acute and chronic isoproterenol-infused rats. Cardiovasc Res 65, 230-238.

Zhang J, Knapton A, Lipshultz S, Weaver J & Herman E. (2008). Isoproterenol-induced cardiotoxicity in sprague-dawley rats: correlation of reversible and irreversible myocardial injury with release of cardiac troponin T and roles of iNOS in myocardial injury. Toxicol Pathol 36, 277-278(a).

Zhang P, Hu X, Xu X, Fassett J, Zhu G, Viollet B, Xu W, Wiczer B, Bernlohr D, Bache R & Chen Y. (2008). AMP activated protein kinase-alpha2 deficiency exacerbates pressure-overload-induced left ventricular hypertrophy and dysfunction in mice. Hypertension 52, 918-924(b).

Zhao Y, Okuyama M, Hashimoto H, Tagawa Y, Jomori T & Yang B. (2010). Bezafibrate induces myotoxicity in human rhabdomyosarcoma cells via peroxisome proliferator-activated receptor alpha signaling. Toxicol In Vitro 24, 154-159.

Zhou Y, Grayburn P, Karim A, Shimabukuro M, Higa M & Baetens D. (2000). Lipotoxic heart disease in obese rats: implications for human obesity. Proc Natl Acad Sci USA 97, 1784-1789.

Zoll J, Monassier L, Garnier A, N'Guessan B, Doutreleau S, Mettauer B, Veksler V, Piquard F, Ventura-Clapier R & Geny B. (2006). ACE inhibition prevents myocardial infarction-induced skeletal muscle mitochondrial dysfunction. J Appl Physiol 101, 385-391.

Zong H, Ren J, Young L, Pypaert M, Mu J, Birnbaum M & Shulman G. (2002). AMP kinase is required for mitochondrial biogenesis in skeletal muscle in response to chronic energy deprivation. Proc Natl Acad Sci USA 99, 15983-15987.

7. APPENDICES

1. Gelatine cubes recipe

8g gelatine

17g sugar

5ml Bovril

100ml water

The solution above was mixed with fenofibrate powder at quantities appropriate to achieve the targeted dose and was then stored at 4˚C.

2. RT-PCR

cDNA synthesis

1. Thaw all necessary components and place them on ice

   Briefly centrifuge all reagents before starting

   Keep all reagents on ice after thawing

2. Pipet in a thin walled-walled RNase- and DNase-free PCR tube, on ice:

   Total mRNA: 10µl

   H_20, PCR grade: 2µl

   Anchored-oligo (dT) 18 primer: 1µl

3. Incubate at 65˚C for 10min and place the tube immediately on ice

4. Add the following components:

   Transcriptor RT Reaction Buffer: 4µl

   Protector RNase Inhibitor: 0.5µl

Deoxyribonucleotide Mix: 2µl

Transcriptor Reverse Transcriptase: 0.5µl

5. Mix well by pipetting

6. Spin the tube briefly in a microfuge

7. Incubate at 55˚C for 30min

8. Incubate at 85˚C for 5 min

9. Place the tube on ice, store in -20˚C freezer

Experiment

Mastermix 1= 14µl enzyme, tube 1a into reaction mix, tube 1b (tube 1a & b in SYBR green kit)

Mastermix 2

For one sample:

H_2O: 12µl

Forward primer: 1µl

Reverse primer: 1µl

Mastermix 1: 4µl

18µl of mastermix 2 added to 2µl cDNA sample

The experiments are then ran in a light-cycler PCR machine

3. Electron Microscopy

Fixation:

Fix in 2.5% gluteraldehyde and 2% paraformaldehyde in PBS pH 7.3 for 1 hour

Cut specimens into small pieces (3×1mm)

Continue to fix for a further 2 hours or overnight

Rinse in PBS for at least 2× 30mins but may be left in buffer in fridge for a week

Postfix in 1% osmium tetroxide for 1 hour

Rinse in PBS overnight, may be left fridge in buffer for about a week

Dehydration and embedding:

50% alcohol for 15mins

70% alcohol for 15mins

80% alcohol for 15mins

95% alcohol for 15mins

100% alcohol for 2× 15mins

Propylene oxide for 2× 20mins

50% propylene oxide/ 50% resin (see below) for 1 hour

Resin overnight

Resin with accelerator (DMP30) for 1 hour

Embed in fresh resin with DMP30- leave at room temperature overnight

Leave at 60˚C for 48 hours

Ready for sectioning

Resin mix:

5.62g Araldite

7.75g Epon 812

15g DDSA

Mix well on rotating mixer

For use add accelerator

Add 0.71g DMP 30

Staining of grids:

Uranyl acetate- saturated solution in methanol

Spin down for 10mins at 3000rpm

Stain for 3mins

Rinse in 50% methanol

Allow to dry

Lead citrate- 1% aqueous solution + 4% conc NaOH (i.e. 1ml NaOH/25ml 1% lead citrate)

Stain for 2mins

Rinse in dilute NaOH (1 drop/50ml)

Rinse in 3× in distilled water

Allow to dry

View on a transmission electron microscopy